



Universidad Autónoma
de Madrid

Biblos-e Archivo
Repositorio Institucional UAM

Repositorio Institucional de la Universidad Autónoma de Madrid
<https://repositorio.uam.es>

Esta es la **versión de autor** del artículo publicado en:
This is an **author produced version** of a paper published in:

Soil Biology and Biochemistry 146 (2020): 107824

DOI: <https://doi.org/10.1016/j.soilbio.2020.107824>

Copyright: © 2020 Elsevier Ltd.

El acceso a la versión del editor puede requerir la suscripción del recurso
Access to the published version may require subscription

1 **Land degradation effects on composition of pioneering**
2 **soil communities: an alternative successional sequence**
3 **for dryland cyanobacterial biocrusts.**

4 Roncero-Ramos B.^{1*}, Muñoz-Martín M.A.², Cantón Y.^{1,3}, Chamizo S.^{1,3}, Rodríguez-Caballero
5 E.^{1,3}, Mateo P.²

6 ¹ Agronomy Department, University of Almeria, Almeria, Spain.

7 ² Biology Department, Universidad Autónoma de Madrid, Madrid, Spain.

8 ³ Centro de Investigación de Colecciones Científicas de la Universidad de Almería
9 (CECOUAL), University of Almería, Almería, Spain

10 *Corresponding author. Email: bea.ron.ram@gmail.com/brr275@ual.es

11 **Abstract**

12 In drylands, soil surfaces in interplant spaces are usually covered by biocrusts, which consist of
13 communities of heterotrophic and chemoautotrophic bacteria, cyanobacteria, mosses, lichens,
14 microalgae, fungi and other organisms. Cyanobacteria are of special interest because of their
15 capacity to promote biocrust succession or increase soil fertility and stability. Therefore, some
16 studies have analyzed their communities in different ecosystems, focusing on how different
17 factors, such as temperature or altitude, influence their composition. Nevertheless, to our
18 knowledge, the relationship between ecosystem degradation and cyanobacterial community
19 composition has not yet been studied in depth. This could be determinant for the successful
20 development of tools for restoring degraded biocrusts by cyanobacterial inoculation. Thus, the
21 objective of this study was to analyze the effect of the ecosystem degradation level on
22 cyanobacteria composition from topsoil communities, where they are keystone pioneering
23 organisms. To do this, we analyzed the cyanobacterial diversity by molecular sequencing (16S
24 rRNA gene) of the DNA extracted from biocrusts at different developmental stages, which were
25 collected from three ecosystems in southeastern Spain. The selected ecosystems represent
26 different “land-condition” states as a result of degradation processes. In one of them soil was
27 removed by mining (the Gádor quarry), the second is a natural badland area (El Cautivo) where
28 water erosion is intense, and the third ecosystem is a well-preserved area (Balsa Blanca). Our
29 findings show that cyanobacterial richness decreases (up to 28 OTUs) as degradation increases
30 and biocrust developmental stage decreases. Also, the relative abundances of most of the
31 species were significantly correlated with the degradation state of the sampling site, either

showing a positive or negative trend. Two of the species which increased in abundance with site degradation, and were especially abundant in incipient biocrusts, were *Leptolyngbya frigida* and *Trichocoleus desertorum*, while other species, also showing an increase in abundance with degradation, but having a higher relative abundance in most developed biocrusts, were *Nostoc commune*, *Tolypothrix distorta* and *Scytonema* sp. The significant correlation of these species with degradation at different biocrusts developmental stages, suggests an alternative developmental sequence for drylands, at least in more degraded ecosystems. In less degraded ones, the composition of the major cyanobacterial groups followed the common pattern of bundle-forming cyanobacteria (54.7 %) pertaining to the *Microcoleus* genus followed by other non-heterocystous filamentous (17.4 %), unicellular/colonial (7.5 %) and heterocystous cyanobacteria (1.1 %). In comparison, the cyanobacterial groups dominating the most incipient biocrusts, colonizing the most degraded soil, were the filamentous non-heterocystous (50.7 %) and the bundle-forming cyanobacteria (48.9 %). Therefore, our results show that some cyanobacterial species, which do not belong to traditional pioneer genera, are frequent colonizers of degraded soils, and then, they could be potentially used for producing a more efficient inoculum for inducing biocrust formation and restoring degraded soils. Finally, it is also remarkable that *L. frigida* appears as dominant in some biocrusts from drylands (up to 74.9 % of abundance) being therefore demonstrated its wide distribution in nonpolar biomes and its capacity to also inhabit degraded arid soils.

Keywords: Biocrust development, degradation gradient, semiarid, cyanobacterial communities, Illumina sequencing

Introduction

Cyanobacteria are the most ancient phototrophic organisms on Earth and first colonizers of soils (Zavarzina and Zavarzin 2013). These prokaryotic microbes inhabit a wide range of biomes from hyper-arid to polar regions (Kumar and Adhikary 2014) in illuminated areas, performing oxygenic photosynthesis with water as the electron donor (Whitton and Potts 2012). In drylands, they are often found in close association with soil particles as part of biological soil crusts or biocrusts, which cover around 12.2% of the Earth surface (Rodríguez-Caballero et al. 2018). These are communities of bacteria (cyanobacteria, chemoautotrophic and heterotrophic bacteria), archaea, algae, fungi, lichens, bryophytes and microarthropods inhabiting on or within the top few centimeters of the soil surface (Belnap et al. 2016). Biocrusts are an essential part of the ecosystems in which they occur, contributing strongly to dryland ecosystem functions, e.g. as major players in the fixation of atmospheric carbon and nitrogen (Rodríguez-Caballero et al. 2018), regulating water fluxes (Chamizo et al. 2016; Cantón et al. 2020) and reducing water and

wind erosion (Zhang et al. 2006; Cantón et al. 2014). In addition, the fixed carbon is used by heterotrophic decomposers and can be stored in the soil (Belnap et al. 2016), whereas the fixed N₂ can be modified by nitrification and denitrification processes at different rates depending on the biocrust community composition (Maier et al. 2018).

Cyanobacteria are a key component of biocrust communities, as they facilitate the establishment of more developed organisms, such as lichens or mosses, and thus the development of later successional biocrusts (Dojani et al. 2011). Their success in colonizing regions with severe environmental conditions, such as drylands, is due to specific features, e.g., their capacity to excrete exopolysaccharides (EPS) to reduce moisture loss around cells (Rossi and De Philippis 2015) and aggregate soil particles (Garcia-Pichel and Wojciechowski 2009; Rossi et al. 2018), adapt their metabolism to successive hydration-desiccation cycles or enter in a dormant state during drought (Rajeev et al. 2013). Some taxa can also fix atmospheric N₂ (Schopf 2013) and/or produce sunscreen-pigments such as scytonemin (Garcia-Pichel and Castenholz 1991).

Due to their benefits to soil functions and their positive influence on succession, a new technology is being developed for dryland soil restoration by cyanobacterial inoculation (Rossi et al. 2017). Many studies have proved their feasibility for inducing the formation of biocrusts on inoculated soils (Hu et al. 2002; Acea et al. 2003; Chen et al. 2006) and their capacity to improve soil properties, such as carbon sequestration (Muñoz-Rojas et al. 2018), nitrogen and EPS content (Román et al. 2018; Mugnai et al. 2018) and soil stability (Chamizo et al. 2018). Studies have also emphasized the importance of taking the biocrust cyanobacterial community composition of the soils to be restored into account so native strains adapted to local conditions can be selected as inoculants (Velasco Ayuso et al. 2017; Giraldo-Silva et al. 2018).

The cyanobacterial community composition in natural biocrusts has been characterized in drylands around the world, such as the Arctic and Antarctica (Jung et al. 2018), Europe (Büdel et al. 2014), the hyper-arid Atacama Desert (Baumann et al. 2018), Southwestern United States (Mogul et al. 2017), Australia (Chilton et al. 2017) and Africa (Maier et al. 2018). In addition, several studies have analyzed how the cyanobacterial community composition is influenced by different climate change-driven environmental factors, such as a temperature increase (Garcia-Pichel et al. 2013; Muñoz-Martín et al. 2019) or changes in precipitation patterns (Fernandes et al. 2018); and gradients in altitude (Capkova et al. 2016) or latitude (Williams et al. 2016). It has been found that cyanobacteria geographical distribution is strongly linked to their ecophysiological characteristics, even at a species level, e.g., whereas more thermotolerant species, such as *Microcoleus steenstrupii*, dominate biocrust communities in hotter deserts *M. vaginatus*, is more abundant in cooler deserts (Garcia-Pichel et al. 2013). There are also anthropogenic factors affecting the cyanobacterial community composition, such as human

induced climate change and land-use intensification (Dojani et al. 2014). For example, it has been described that trampling biocrusts causes a decrease in the proportion of cyanobacteria in the microbiome (Kuske et al. 2012) and a change in their composition, reducing diazotrophic species while increasing non-heterocystous filamentous cyanobacteria, such as *M. vaginatus* (Steven et al. 2018). However, further information concerning the influence of ecosystem degradation on cyanobacteria community composition of biocrusts is desirable, especially to successfully restore them. Knowing which cyanobacteria colonize soils at different degradation levels would help selecting the inoculants that could successfully cope with stressful conditions typical of a particular degraded area, such as high erosion or insolation.

This study analyzed the cyanobacterial community composition of biocrusts sampled at three study areas in southeastern Spain, along a gradient of land-condition representing different degradation levels, from highest to lowest, as follows: a limestone quarry after active mining (Gádor quarry), a badlands landscape under intense historical erosion (El Cautivo) and a well-preserved steppe ecosystem (Balsa Blanca). We hypothesized that the cyanobacterial community composition would change within the degradation gradient towards a more incipient stage dominated by pioneer cyanobacterial species as degradation increases.

Materials and Methods

Study areas description

Three experimental areas located in southeaster Spain and characterized by a semiarid Mediterranean climate, were selected to study cyanobacteria communities composing cyanobacteria-dominated biocrusts. The selected areas represented three ecosystems with different degradation levels, and were chosen with the objective of analyzing how cyanobacteria communities could change along a degradation gradient. The most disturbed one, in this case due to active mining, is a limestone quarry (Gádor quarry, 36°55'20" N, 2°30'29" W). This site has a mean annual temperature of 17.6°C, an absolute minimal temperature of -2.6°C and maximal of 42.7°C (Luna et al. 2016). The mean annual precipitation and air relative humidity are, respectively, 206 mm and 66%. Before mining, the soil surface was covered by patches of *Macrochloa tenacissima* (L.) Kunth with cyanobacteria, lichens and mosses biocrusts in the interspaces and under plant canopy. Although the unaltered soils surrounding the quarried areas are, in most cases, Epileptic and Endoleptic Leptosols and Calcaric Regosols (García-Ávalos et al. 2018), the edaphic characteristics of the substrate in the sampled area are determined by the reclamation operations of The Cement Factory of Gádor (Almería, Spain), consisting of the construction of artificial hillslopes by means of covering the spoil bank with a layer of overburden substratum mainly from upper Miocene marls. The topography of

end- of- exploitation quarries has been reshaped, but rills and gullies cover most of the surface, because of the intense water erosion processes. The quarried rock is essentially a calcareous sandstone, which overlays a calcitic mudstone (marls) also partially quarried. Sampling sites rest on the marls, and consist of a substrate with poor soil development, especially in the areas closer to the active mining activities, and with many properties of these soils inherited from the parent material. Dominant soil texture is silty, average pH is 8.4, and organic carbon and nitrogen contents are very low and calcium carbonate content is around 36% (Luna et al. 2016).

The selected ecosystem representing the intermediate level of degradation is El Cautivo experimental area (Tabernas desert natural reserve, 37°00'38.6" N, 2°26'30.2" W), a badlands landscape, developed on a highly erodible mudstone. This system is subjected to geologic water erosion processes, reaching rates (up to 280 ton ha⁻¹ in one event) much higher than in surrounding areas with other lithologies (Cantón et al. 2001). In addition, open and exposed areas are also subjected to wind erosion. Soil classifications in the sampling area correspond to Epileptic, Endoleptic or Calcaric Regosols (Cantón et al. 2003). The mean annual precipitation is 235 mm and the mean annual temperature is 18°C (Cantón et al. 2014). The absolute minimum and maximum annual temperatures are, respectively, -5.5 and 45°C. Also, the mean air relative humidity is 60%. This area is partially covered by *M. tenacissima* (L.) Kunth and other vascular plants, and in the interplant spaces there are different types of biocrusts, dominated mainly by lichens, such as *Diploschistes diacapsis*, *Squamarina lentigera* or *Lepraria crassissima* (Lázaro et al. 2008), and cyanobacteria at different developmental stages, as previously described (Cantón et al. 2004; Chamizo et al. 2012). Soil development in general may vary from low to moderate depending on the landform. Soil texture is mainly silty and silty loam, pH is 7.8 and calcium carbonate content of 26% (Chamizo et al. 2012).

The third ecosystem is a well-preserved, protected area within the Cabo de Gata Natural Park, the Balsa Blanca experimental site (36°56'26.0" N, 2°01'58.8" W). This is a steppe ecosystem with a mean annual precipitation of 220 mm and a mean annual temperature of 18°C (Mora and Lázaro 2013). The absolute minimum and maximum annual temperatures are -1.3 and 39.8°C. The mean air relative humidity is 68%. Soils are classified as Mollic Lithic Leptosols (Calcaric) (Mora and Lázaro 2013) and their surfaces are partially covered by vegetation dominated by *M. tenacissima* (L.) Kunth. Interplant spaces are colonized by biocrusts, which are mainly composed by cyanobacteria, and late-successional lichens, mainly *Diploschistes diacapsis* (Miralles et al. 2012), and mosses. Soils, although shallow (10 cm on average), have a more developed structure. Prevailing soils are characterized by a sandy loam texture, saturated in carbonates (Rey et al. 2011) and alkaline, with pH of 8.3 in the interplant spaces (Mora and Lázaro 2014).

Biocrust sampling and classification

Biocrusts were sampled under dry conditions using Petri dishes (90 mm diameter, 10 mm deep) within two consecutive days in February 2016. On each area, from 5 to 8 samples from incipient to developed cyanobacteria-dominated biocrusts were taken, except for the less degraded area, Balsa Blanca, where only developed cyanobacteria-dominated biocrusts were identified. Biocrust development was visually assessed on the field based on previous knowledge of biocrust communities within the sites (see Lázaro et al. 2008; Chamizo et al. 2012) and also coinciding with biocrust development features established by Belnap et al. (2008). Samples were maintained under dry conditions, stored in darkness and at room temperature in the laboratory.

Dissecting microscope (Leica, Leica Microsystems, Wetzlar, Germany) observations allowed us to better classify samples according to their developmental stage, by observing the presence of major groups, such as mosses, lichens, algae or cyanobacterial morphotypes. Biocrusts were classified as follows: from the Gádor quarry area, we obtained incipient (IQ), medium (MQ) and high developed (DQ) biocrusts; from El Cautivo area, incipient (IC) and high developed (DC) biocrusts; and from the Balsa Blanca area, high developed biocrusts (BB). Afterwards, representative subsamples (and with equal size) of the crust layer (2 mm) within each biocrust type for each area, according to microscopic inspection were selected, mixed and mortared to obtain a composite sample in order to include possible patchiness, following the procedure described in previous studies (Muñoz-Martín et al. 2019; Becerra-Absalón et al. 2019).

Characterization of physicochemical soil properties

All samples were air-dried and sieved to 2 mm for the determination of different physical and chemical properties. Soil particle distribution was determined by the Robinson's pipette method. For this, the organic matter of the samples was previously removed with 30% H₂O₂ and agitation in 10 ml of 40% sodium hexametaphosphate (Gee and Bauder 1986). Then, separation of the sand fraction was achieved by wet-sieving, oven drying and dry-sieving. Soil Organic Carbon content (OC) was determined by the Walkley and Black method modified by Mingorance et al. (2007) by measuring the absorbance (590 nm) of the oxidized organic matter in a spectrophotometer (Helios Gamma, Thermo, England). Total N was determined employing a LECO TRUSPEC C/N analyzer. In addition, other soil properties including electrical conductivity, gypsum, micronutrients (zinc, copper, iron and manganese) and base cations (calcium, magnesium, potassium and chloride) were analyzed by Fitosoil S.L following the standardized procedures.

Establishing a land-condition index of each biocrust sampling site

The normalized difference vegetation index (NDVI; Tucker 1979; Eq. 1) is a commonly accepted surrogate for vegetation and biocrust cover, biomass and vitality (e.g. Del Barrio et al. 2010; Rodríguez-Caballero et al. 2015; Gypser et al. 2016) and represents site long-term capacity to sustain biomass (Del Barrio et al. 2010) and can be used to estimate the land-condition index (Del Barrio et al. 2010). The land-condition index represents the level of maturity of the ecosystem in response to a degradation process and has been officially adopted by Spain (Sanjuán et al. 2013) and Portugal (Rosario et al. 2015) to perform land degradation reports to the UNCCD. To assess the land condition (or degradation level) of each sampling site, we used SENTINEL-2 images acquired during a complete hydrological year (2016-17) to estimate the mean annual NDVI for each sampling site and for a reference site in each area (well-preserved locations within the ecosystem representing the climax community under current climate). Using these data, we estimated the land-condition of each sampling site as the mean annual NDVI of an area of 3 x 3 pixels around each sampling site divided by the mean NDVI of the corresponding reference site (Eq. 2). If the capacity of the ecosystem to sustain biomass under certain environmental conditions changes in response to degradation process, and deviates from the mature community found in the same place (reference site), it will be reflected in the index value.

Mean annual SENTINEL-2 NDVI values were obtained from monthly greenest composites using google earth engine.

Eq. 1: $NDVI = (NIR - R) / (NIR + R)$

where NIR and R are, respectively, the reflectance of the near infrared (band 8, 835 nm) and red (band 4, 665 nm) spectral bands of SENTINEL-2.

Eq. 2: Land condition index = $\overline{NDVI}_{biocrust} / \overline{NDVI}_{reference}$

where $\overline{NDVI}_{biocrust}$ is the mean annual NDVI of the location where each composite sample was acquired, calculated as the averaged mean NDVI of the 3 x 3 pixels around each sampling location. $\overline{NDVI}_{reference}$ is the reference value for each study area calculated as the mean annual NDVI of the reference place. Thus, higher values of the index indicate land conditions closer to maturity, whereas low values represent biomass and coverage loss in response to degradation processes.

Genetic analyses of the cyanobacterial communities

Cyanobacterial community composition was analyzed by sequencing the 16S ribosomal RNA (rRNA) gene with Illumina MiSeq. For that, DNA was extracted from three aliquots of 0.33 g of homogenized composite samples with a Powersoil DNA extraction Kit (Mobio Carlsbad, CA,

USA). The protocol was modified at the beginning to successfully break up all cell walls by incubating soil in a homogenization solution followed by three freeze-thaw cycles, as previously described (Muñoz-Martín et al. 2019). These cycles were performed by submerging samples in liquid nitrogen, then heating them up to 60°C and homogenizing them with a pellet pestle using a hand-operated homogenizer (CSB-850-2RET, Bosch, Solothurn, Switzerland). At the end of the protocol, each extraction was eluted in 100 µL of buffer. Finally, the DNA extracted from the three independent samples was mixed for PCR amplification.

The following primers, which are specific for cyanobacteria, were employed to amplify the variable regions V3-V4 of the 16S rRNA gene: CYA359F and 781Ra/781Rb (Nubel et al. 1997) in separate reactions for each reverse primer (Boutte et al. 2006). PCR reactions consisted of 1 x PCR buffer, 1.5 mM of magnesium chloride, 3 ng of DNA and 200 nM of each primer, which were barcoded to each sample. The cycle started with an initial denaturation for 30 s at 98°C, followed by 22 cycles of denaturing at 98°C for 10s, annealing at 54°C for 20s and extension at 72°C for 20s, and the final extension at 72°C for 2 min. The Genomic Service from the Universidad Autónoma de Madrid processed all amplicons (read length of 2 x 300 bp) with a MiSeq sequencer (Illumina Inc., San Diego, CA, USA). The lowest number of sequences obtained was 76,798.

The first step of raw sequences processing was to check their quality using FASTQC v.0.11.3. After that, they were processed employing QIIME v.1.9.0 (Caporaso et al. 2010) with the workflow published by Pylro et al. (2014), based on the UPARSE pipeline (Edgar 2013) with software USEARCH v.8.1. Then, the sequences that could be merged using QIIME default parameters because their forward and reverse sequences overlapped, were filtered by quality with fastq maxee 0.5 and by length, retaining sequences longer than 420 bp. Afterwards, sequences were de-replicated and singletons were discarded. Then, sequences with a similarity higher than 97% were clustered in operational taxonomic units (OTUs) and those with a number of reads lower than 0.005% were discarded, as suggested by Navas-Molina et al. (2013). The first taxonomical assignment was performed against GreenGenes database by the classifier method of the Ribosomal Database Project with a confidence value of 0.8 (Navas-Molina et al. 2013), which allowed the removal of those OTUs identified as chloroplasts or non-cyanobacterial organisms. Then, to achieve a better assignment, OTUs were matched against the sequence dataset of previously isolated and identified cultures from biocrusts in the same sites (Roncero-Ramos et al. 2019), employing the ‘uparse ref command’ in USEARCH (Edgar 2010). Finally, other taxonomic assignments were done by blasting sequences against the National Center for Biotechnology Information (NCBI) database and following the lowest common ancestor (LCA) algorithm in CREST (Lanzén et al. 2012) against the silvaMod database (Yilmaz et al. 2014). Phylogenetic trees were constructed by the neighbor joining

algorithm with MEGA (version 7.0.21; Kumar et al. 2008), including our sequences and those that matched from the different databases employed. We applied the Tajima-Nei model (Tajima and Nei 1984) to calculate the evolutionary distances with a pairwise deletion of gaps and missing data, as well as 1000 replications to estimate the bootstrap phylogeny test (Felsenstein, 1985). % of similarity was calculated as $(1 - p \text{ distance}) \times 1000$. All OTUs sequences are available at Genbank database (accession numbers MK938309 - MK938372). Raw sequencing data have been deposited in the NCBI Sequencing Read Archive under accession number PRJNA542686.

Statistical analyses

For a better visualization of the community composition of each sample, a chord diagram was obtained with the function `chordDiagram` included in the `circlize` package (Gu et al. 2014) in R 3.3.1 (Development Core Team 2017). The dissimilarities among phylotypes found in the samples were calculated using the unweighted pair group method with arithmetic mean (UPGMA) analysis. Community dissimilarities were computed using the weighted-unifrac distance matrix, using the `QIIME` package. This generates a dendrogram depicting the phylotypes relationships among samples.

A χ^2 contingency table (Steel & Torrie 1980) was used to determine whether the relationship between the land-condition index of the biocrust sampling site and the abundance of a certain taxonomic group was statistically significant in each case. The contingency tables were calculated for all the taxonomic assignments (Table 2), using the relative abundance found by adding up the abundances of all the operational taxonomic units (OTUs) in each taxonomic group. This variable was compared with the land-condition index for each sampling site (Eq. 2). This method therefore compared the relative abundance of one taxonomic group to the relative abundance of the rest of species across the range of the index, showing increasing or decreasing trends in relative abundance of each taxonomic group along the land-condition index gradient. To find out whether there was significant dependence between the abundance of a taxonomic group and the land-condition index of the site, the total χ^2 found from the contingency table was divided into two components: 1) a χ^2 testing for a significant linear rate of change of abundance along the index, and 2) a χ^2 test for the significance of the residual variance that remained unexplained by the linear trend (Steel & Torrie 1980, 1985; Snedecor & Cochran, 1984). The existence of trends was determined from these two tests (Pinder et al. 1997; Cantón et al. 2004). The slope parameter (b) of the linear trend was also calculated to determine if the change in abundance increased or decreased with decreasing values of the index (high degradation), which corresponds, respectively, to a positive or negative value.

Results

Degradation gradient across sampling sites

The land-condition index, calculated based on the NDVI of the sites where the biocrusts were sampled, established a clear degradation gradient of samples (Table 1). The lowest land-condition index values were found in the most disturbed area (the Gádor quarry), followed by El Cautivo and the well-preserved ecosystem, Balsa Blanca (Table 1). Moreover, among the biocrust types in each area, incipient biocrusts were located at the sampling sites with an index lower than the sites where the developed biocrusts were sampled in the same area. Therefore, the land-condition gradient is in the order of the ecosystem maturity of each study area and represents the developmental level of the biocrusts sampled in each area. The soil physicochemical properties analyzed, such as organic carbon, total nitrogen content and the C/N ratio, were also in concordance with the land-condition index values, and were higher in sites with a land-condition index close to 1 (Table 1). In general, this was also the case for the availability of K and the micronutrients Mn, Fe and Zn, which followed a similar pattern of increasing availability (Table 1).

General community composition. Taxonomic assignment

Table 2 shows the taxonomic assignments of the OTUs based largely on comparison with the sequences of the cultures previously isolated from these areas and/or blasted and phylogenetic trees dedicated (Figures 1 and 2). Thus, OTU1 was assigned to *Leptolyngbya frigida* and another three OTUs (3, 56 and 64; Table 2) were classified as *Leptolyngbya* sp. since all of them were included in different well-supported clusters in the phylogenetic tree belonging to this genus (Figure 1a). Furthermore, OTU1 clustered with sequences corresponding to isolated cultures from El Cautivo and Gádor quarry biocrusts, previously identified as *L. frigida* (Cluster V; Figure 1b) (Roncero-Ramos et al. 2019). Other filamentous non-heterocystous cyanobacteria were *Oculatella* (OTU18 and 53) and *Phormidium* (OTU33) (Table 2). OTUs belonging to the *Oculatella* genus clustered together with other sequences from the databases in Cluster VII (Figure 1a), and one of them was taxonomically assigned to *O. kazantipica*, as it showed 98.1% similarity with a sequence from isolated cultures of biocrusts from Las Amoladeras (Cluster VII; Figure 1b), a study area very near and similar to Balsa Blanca (Roncero-Ramos et al., 2019).

Of the bundle-forming cyanobacteria, OTU2 was identified as *Trichocoleus desertorum*, which was included in Cluster VI (Figure 1b) with OTU21 and other sequences, especially two belonging to cultures previously isolated from biocrusts from El Cautivo (Roncero-Ramos et al. 2019), supporting its taxonomical assignment (Table 2). The other bundle-forming genus identified, *Microcoleus*, was assigned to twenty OTUs, included in several clusters along the

phylogenetic tree (Table 2; Figure 1a). One OTU could be taxonomically assigned to *M. vaginatus* (OTU4), included in a consistent cluster (II; Figure 1b); and other OTUs to *M. steenstrupii* (OTUs 8, 13, 23, 25, 42, 50 and 55), included in different clusters with sequences identified as this species, especially one belonging to an isolated culture from El Cautivo biocrusts (Roncero-Ramos et al. 2019), which is 99% similar to OTU8 (Table 2; Cluster IV, Figure 1b). Finally, OTU49 was assigned to *M. paludosus*, as it clustered with this taxon in the phylogenetic tree (Figure 1a) and presented high similarity (99.8%) with a sequence previously identified as this species (Table 2).

The unicellular/colonial group was composed of 14 OTUs dominated by the *Chroococcidiopsis* genus (Table 2) and represented by 13 OTUs located in ten clusters along the phylogenetic tree (Figure 1a). The other genus identified was *Pleurocapsa*, represented by OTU62 (Figure 1a, Table 2).

The heterocystous group was composed of OTUs of typical biocrust genera: *Scytonema*, *Tolypothrix*, *Nostoc*, *Mojavia*, and *Macrochaete*. *Scytonema* was represented by four OTUs (9, 22, 38 and 61) grouped in three different clusters (Figure 2). Two of those clusters corresponded to two divergent operons of *Scytonema hyalinum*, including OTU 9 and 22, and taxonomically assigned to previously identified strains isolated from biocrusts in El Cautivo and Las Amoladeras (Roncero-Ramos et al. 2019) (VI and VIII, Figure 2; Table 2). In Cluster VII, several sequences from the databases assigned to *Scytonema* sp. were found with OTUs 38 and 61 (Figure 2). OTU15 was taxonomically assigned to *Tolypothrix distorta*, which was included in the same cluster with sequences from cultures isolated from El Cautivo and the Gádor quarry (Roncero-Ramos et al. 2019) (Table 2; Cluster III, Figure 2). *Nostoc*, represented by OTU16, identified as *N. commune*, was placed in Cluster I (Figure 2) with other sequences from the databases, as well as from cultures isolated from biocrusts in the Gádor quarry (Roncero-Ramos et al. 2019). OTU 63 was assigned to *Mojavia* sp, a genus morphologically similar to *Nostoc* (Řeháková et al. 2007), clustering with several sequences from the database and one belonging to biocrusts from Aranjuez, another Mediterranean semiarid area (Cano-Díaz et al. 2018) (Cluster II, Figure 2). *Macrochaete lichenoides* (OTUs 24), was included in Cluster IV with sequences of this cyanobacterium from the database (Figure 2).

Changes in the cyanobacterial community structure and richness along the degradation gradient

The dominant taxa differed by area and biocrust developmental stage (Figures 3 and 4). The bundle-forming cyanobacteria were abundant in incipient biocrusts, decreasing as the developmental stage increased (Figure 4). The heterocystous forms then tended to be more

abundant, except for the developed biocrusts in Balsa Blanca, where bundle-forming cyanobacteria were still the dominant group (Figure 4). Unicellular/colonial cyanobacteria tended also to be more abundant in developed than in incipient biocrusts (Figure 4). Other filamentous non-heterocystous cyanobacteria showed no specific tendency regarding the developmental stage (Figure 4). The most abundant genus in the incipient biocrusts on the post-mining soil at the Gádor quarry was *Leptolyngbya*, (50.5%), with 23.6% of the reads assigned to *L. frigida*, followed by *Trichocoleus desertorum* (32.5%), *Microcoleus vaginatus* and *Microcoleus* sp. (8.3 and 7.7% respectively) (Figure 3). These biocrusts (IQ) were composed almost entirely by filamentous non-heterocystous cyanobacteria (99.6%), of which 48.9% of the total reads were bundle-forming, and 50.7% non-bundle-forming (Figure 4). The medium developed biocrusts from the Gádor quarry (MQ) were also dominated by filamentous non-heterocystous cyanobacteria (78.2%), and only 2.9% of the reads were bundle-forming, while the unicellular/colonial cyanobacteria were as high as 21.4% (Figure 4). The dominant taxa in these biocrusts was also *L. frigida* (74.9%), followed by *Chroococcidiopsis* sp. (21.4%) and *T. desertorum* (2.5%) (Figure 3). However, in the developed biocrusts from the Gádor quarry (DQ), heterocystous cyanobacteria were up to (42.8%), with fewer filamentous non-heterocystous and unicellular/colonial down to 46.2% (of which 6.6% were bundle-forming species) and 9.3%, respectively (Figure 4). At the species level, the dominant abundance was again *L. frigida* (36.9%), followed by the heterocystous cyanobacteria: *S. hyalinum* (16.2%), *T. distorta* (15.0%) and *N. commune* (11.3%) (Figure 3). The unicellular/colonial group was mainly represented by *Chroococcidiopsis* spp. (9.3%), and the most abundant bundle-forming species was *M. steenstrupii* (5.3%).

All biocrusts from El Cautivo, also subjected to intense natural erosion, but representing an ecosystem not as intensively degraded as the Gádor quarry, showed a similar composition. However, some differences were found in the proportion of each taxon in the two types of biocrusts (Figures 3 and 4): i) Incipient biocrusts from El Cautivo (IC) were dominated by the filamentous non-heterocystous group (60.5%), among which 46.9% of the reads were bundle-forming (Figure 4), corresponding to *Microcoleus* spp., represented by *M. vaginatus* (17.2%), *M. steenstrupii* (15.5%) and *Microcoleus* sp. (8.9%) (Figure 3), while 21.2% of the reads were assigned to *Chroococcidiopsis* spp. Other cyanobacteria which were highly abundant in the Gádor quarry, such as *L. frigida* and *T. desertorum*, were reduced to 4.2 and 5.2%, respectively. As biocrust development increased (DC), the *Chroococcidiopsis* spp. unicellular/colonial cyanobacteria (50.6 %) replaced the filamentous non-heterocystous group reducing the bundle-forming cyanobacteria to 15.0% (Figures 3 and 4).

Finally, and contrary to expectations, we found that the filamentous non-heterocystous group (72.1%), mainly composed of bundle-forming cyanobacteria (54.7%; Figure 4), was dominant

in developed biocrusts from the well-preserved study area (Balsa Blanca). In this area, the heterocystous and unicellular/colonial groups were in low abundance (7.5 and 1.1%, respectively) (Figure 4). The *Microcoleus* genus, composed of *M. steestrupii* (22.2%), *Microcoleus* sp. (18.6%), *M. vaginatus* (11.3%) and *M. paludosus* (0.3%), was the most abundant one (52.4%) (Figure 3). Other species with an abundance over 2% were *Oculatella kazantipica*, which was also more abundant than in the rest of the samples (6.0%), and *S. hyalinum* (5.4%; Figure 3).

Cyanobacterial richness may be observed in Figure 5, which shows the total number of OTUs at each sampling site and type of biocrust. This is not clearly visible in Figure 3, because the OTUs with very low abundance are not labeled. The richest biocrust was found in the well-preserved location, Balsa Blanca, with 59 OTUs (Figure 5). A general downward trend in the number of phylotypes was found with increased degradation, being the minimum number of OTUs found 31, in incipient biocrusts of the Gádor quarry (IQ; Figure 5).

Influence of the degradation level on cyanobacterial community composition

The land-condition index (or degradation level) and the relative abundance of each taxonomic group per sampling site showed a significant relationship in all cases, except for the unicellular/colonial cyanobacteria, *Chroococcidiopsis* sp. and *Pleurocapsa* sp. (Figure 6). The χ^2 test confirmed this association between the relative abundance of most of the taxonomic groups in the cyanobacterial biocrust community and site degradation level. Moreover, each group behaved differently as degradation decreased, as shown by the slope parameter (b) of the linear trend (Figure 6). According to the results showed in Figure 3 and 4, different cyanobacterial community structures were found in sites with different degradation levels (Figure 6). *L. frigida*, *Leptolyngbya* sp., *T. desertorum*, *Scytonema* sp., *T. distorta* and *N. commune* had a negative slope, meaning that their abundance decreased as the land-condition index increased. In other words, the abundance of these species increased in more degraded sampling sites (Figure 6). The abundance of the rest of species, among which we can highlight the presence of all *Microcoleus* spp. and the heterocystous cyanobacteria *S. hyalinum* and *Macrochaete lichenoides*, showed, in contrast, a significant positive slope parameter. This means that their abundance increased as land-condition improved (Figure 6). Furthermore, some differences between species belonging to the same genus were detected, such as a higher value on the linear regression slope of *M. vaginatus* in comparison with *M. steenstrupii* (Figure 6). The influence of land-condition on cyanobacterial community composition of biocrusts was also corroborated by a UPGMA analysis (Figure 6). This analysis showed that differences in richness and composition among sampling sites influenced their ordination, according to dissimilarities of phylotypes found in the samples (Figure 6). The most distant were the

incipient biocrusts from the Gádor quarry, while the rest of samples were included in the same cluster, but in different groups by study area (Figure 6).

Discussion

Changes in the cyanobacterial community composition and richness along the degradation gradient

It is well known that the cyanobacterial community composition in biocrusts is influenced by factors such as climate, soil properties, location or development (Garcia-Pichel et al. 2013; Capkova et al. 2016; Chilton et al. 2017). In this study, we have also found changes in the cyanobacterial community composition along a degradation gradient, whereby shifts in taxa representative of the study areas were observed in relation to the land-condition index (or degradation level) (Figure 6). As expected, this index was higher in the well-preserved study area, Balsa Blanca, and decreased as disturbance of the ecosystem increased, with the lowest values in post-mining soils from the Gádor quarry. In addition, the land-condition index showed differences among the sampling sites within each ecosystem, with more developed cyanobacterial biocrusts at locations where the index was higher (Table 1). The change of the cyanobacterial community composition along the degradation gradient may have implications on ecological processes specifically carried out by different cyanobacteria in biocrusts, such as water retention (Chamizo et al. 2017; Adessi et al. 2018), reduction of soil and nutrients loss (Chamizo et al. 2012; Cantón et al. 2014) or soil fertility increase (Beraldi-Campesi et al. 2009). Therefore, if the new cyanobacterial community composition has different functions in the ecosystem, it may synergistically increase the negative impacts already associated to the degradation processes.

In addition, the degradation gradient is also in agreement with soil physicochemical properties of the sampling sites, as revealed the increase in OC, N and the C/N ratio (Table 1) with the land-condition index and cyanobacterial biocrust development. Thus, the highest OC and N contents and C/N ratio were found in the well-preserved ecosystem (Balsa Blanca) and decreased as degradation increased in El Cautivo and the Gádor quarry. This decrease may be caused by the relative prevalence of geochemical control on nutrient cycling and erosion (Delgado-Baquerizo et al. 2013). Micronutrients availability, which are critical for cell growth, redox homeostasis and as enzyme cofactors in photosynthesis and other biochemical pathways (Welch et al. 1995), were, in general, also positively related with the land-condition index (Table 1). All soils were alkaline (pH values ranging between 7.8 and 8.4) and the clay content increased with degradation (Table 1). Therefore, the higher available Cu, Fe, Mn or Zn concentration found in the well-preserved site, may be related with a high EPS production by

cyanobacteria, which could be also linked with the high OC content in the less degraded sites (Table 1). These EPS could be also playing an important role forming soluble complexes with Cu, Fe, Mn or Zn increasing their bioavailability (Moreno-Jimenez et al. 2019). The degradation affects these micronutrients, becoming less available, through the deterioration of soil properties such as the decrease of OC.

In addition to the differences found in cyanobacterial community composition among areas and biocrust developmental stages, an overall decrease was found in cyanobacterial richness with increased ecosystem degradation (Figure 5), both of which influenced the ordination of samples according to the phylotypes dissimilarities (Figure 6). A similar decrease in cyanobacterial richness has been previously reported in disturbed biocrusts with regard to land use (Dojani et al. 2014), and in earlier biocrust developmental stages compared to more developed ones (Chilton et al. 2017). Moreover, the richest biocrusts, and those in their most mature developmental stage were those inhabiting the well-preserved ecosystem at Balsa Blanca. The highest soil organic carbon and total nitrogen content, which has been previously correlated with cyanobacterial richness, were also found here (Williams et al. 2018). A previous study (Miralles et al. 2012) found an increase in soil organic matter quality (higher abundance of more recalcitrant carbon compounds) in more developed than in less developed biocrusts in both Balsa Blanca and El Cautivo, also correlated with an increase in soil bacterial richness (Siciliano et al. 2014). Therefore, our data shows a decrease in cyanobacterial richness with an increase in degradation, which suggests a regression in the community developmental stage that corresponds with our visual estimation of biocrusts development.

An alternative successional sequence for dryland biocrusts

It is traditionally assumed that in early stages of biocrust development, communities are usually dominated by bundle-forming cyanobacteria, mainly *Microcoleus* spp. (Garcia-Pichel et al. 2001). The ability to build rope-like bundles of trichomes that remain held together in a common extracellular EPS sheath, allows them to colonize physically unstable soils, which contributes significantly to the biostabilization process (Garcia-Pichel and Wojciechowski 2009), thus inducing the formation of an incipient biocrust. Moreover, *M. vaginatus* releases a wide range of metabolites into the environment (Baran et al. 2015), which promotes the colonization of soils by later-successional organisms under favorable environmental conditions. However, evidence from this study shows that all biocrusts from the most degraded area, the Gádor quarry, were dominated instead by the non-bundle forming genus *Leptolyngbya*, especially *L. frigida* (Figure 3). This is also supported by the strong significant negative relationship of *Leptolyngbya* sp. with the land condition index, in other words its abundance increases with the degradation level, in contrast to the performance of *Microcoleus* sp., whose

abundance decreases with degradation (Figure 6). Furthermore, this negative trend with degradation was more intense depending on the *Microcoleus* species, e. g. *M. vaginatus* was less affected than *M. steenstrupii* (Figure 6). *Leptolyngbya* spp. are found in almost every type of ecosystem and are recognized for their ability to withstand extreme conditions, such as heavy-metal polluted water (Podda et al. 2014). It can also colonize polar environments and, in fact, was considered an Antarctic endemism (Taton et al. 2006), until it was found in other sites, such as the Arctic (Jungblut et al. 2009), South Africa (Dojani et al. 2014), Mediterranean ecosystems (Muñoz-Martín et al. 2019), and also in biocrusts in the quarry of this study (Roncero-Ramos et al. 2019). Moreover, to our knowledge, this is the first report of biocrusts from semiarid areas dominated by *L. frigida*, which support wide distribution in nonpolar biomes. In addition, it should be noted that the bundle-forming cyanobacterium, *Trichocoleus desertorum*, was also highly abundant in incipient biocrusts from this site (Figure 3) and tended to be more abundant with increasing degradation (Figure 6). Thus, it could replace the functional role in soil stabilization of typical *Microcoleus* spp. *T. desertorum* had previously been identified in more arid environments, such as the hyper-arid Atacama Desert (Mühlsteinová et al. 2014), and as a less abundant component of biocrusts along a temperature gradient in Spain (Muñoz-Martín et al. 2019). Therefore, *Leptolyngbya* spp. and *T. desertorum*, able to cope with extreme conditions, could be the first colonizers of substrates with scarce edaphic development or very degraded soils, enabling subsequent colonization by other species.

On the contrary, following the general pattern described in the literature to date, incipient biocrusts from a less degraded area, El Cautivo, and well-developed biocrusts from the most preserved site, Balsa Blanca, were both dominated by bundle-forming cyanobacteria, such as *M. steenstrupii*, *M. vaginatus*, and other *Microcoleus* spp. (Figures 3-4). As these are less degraded sites in comparison with the Gádor quarry, such results suggest that these bundle-forming cyanobacteria may require a certain level of edaphic development and stability to successfully colonize them. Thus, explaining why they are not dominant in the incipient biocrusts inhabiting substrates with hardly edaphic development, such as all biocrusts in the Gádor quarry site. The relatively high abundance of *Chroococcidiopsis* spp. is noticeable in medium-developed biocrusts from the Gádor quarry area and in the developed biocrust from El Cautivo. However, their abundance did not follow a significant trend in relation with the land-condition index (Figure 6). In El Cautivo, developed biocrusts are usually colonized by lichens, such as *Squamarina* or *Collema* spp. (Lázaro et al. 2008), and although we selected those dominated by cyanobacteria, some lichens were also present (see images in Figure 6). Thus, we could have sequenced their photobionts, which in drylands are commonly unicellular/colonial cyanobacteria (Crittenden et al. 2007). In fact, one of the phylotypes found was 99.8% similar to a *Chroococcidiopsis* sp. sequence, which has been reported to be a lichen photobiont (Fewer et

al. 2002). However, less abundance of this taxon was observed in biocrusts from the less degraded area, Balsa Blanca, which were also dominated by lichens. *Chroococcidiopsis* spp. has previously been identified in biocrusts from very arid environments, such as the Atacama Desert or the Arctic (Patzelt et al. 2014; Pushkareva et al. 2015), to less extreme ecosystems (Muñoz-Martín et al. 2018; Williams et al. 2016). Furthermore, its presence has been related to more developed biocrusts (Yeager et al. 2004) and nitrogen fixation (Fewer et al. 2002). Therefore, the occurrence of *Chroococcidiopsis* spp. in these biocrusts can contribute to the nutrient cycling through the nitrogen fixation carried out by these cyanobacteria.

Heterocystous cyanobacteria, which are commonly found in later stages of biocrust succession (Weber et al. 2016), clearly increased in the developed biocrusts from the Gádor quarry, with high abundance of *S. hyalinum*, *T. distorta* and *N. commune* (Figure 3). It is also remarkable that *S. hyalinum* significantly decreased with land-condition, showing an opposite trend in comparison with *T. distorta*, *N. commune* and *Scytonema* sp. (Figure 6). These species have been previously identified in many biocrusts worldwide, such as in North America or Africa (Yeager et al. 2007; Dojani et al. 2014) where they play an important role in increasing soil fertility by nitrogen fixation (Yeager et al. 2004). Furthermore, they produce UV-screening pigments, such as scytonemin, which decrease the albedo (Couradeau et al. 2016). However, some species, such as *Nostoc* sp. are sensitive to biocrust disturbances (Dojani et al. 2014; Steven et al. 2018). Therefore, these cyanobacteria could have developed the ability to recover from disturbances and becoming active after pioneering organisms colonize the soil and improve its properties. The fact that these cyanobacteria were able to grow in late-successional biocrusts in degraded soils may be related to adaptive strategies for coping with extreme conditions. One of these strategies could be the development of cell survival stages, the akinetes, known only in heterocystous cyanobacteria (Adams and Duggan, 1999). These metabolically inactive cells can remain dormant for years, germinating and developing new filaments when conditions become suitable again. Evidence has shown that *Nostoc* can remain inactive in drylands for months, years, or even several decades, and fully recover its metabolic activity within days or even hours when environmental conditions change (Hu et al. 2012), such as after total desiccation (Becerra-Absalón et al. 2019).

Rehabilitation of degraded soils after disturbance in vulnerable dryland biocrusts is essential to recover the variety of important ecological functions they provide. The results from this study support an alternative successional sequence in which *Leptolyngbya* spp. dominated the first developmental stages of biocrusts of substrates with hardly edaphic development and more degraded soils, along with the bundle-forming *T. desertorum*. These cyanobacteria might have developed strategies for survival under harder conditions, such as higher temperatures and drier, less stable soils. After these cyanobacteria had improved soil properties in the most degraded

sites, the heterocyst-forming cyanobacteria became dominant in later successional biocrusts. The identification of this alternative successional sequence should be considered when studying the development of dryland biocrust communities. Besides, it could contribute to increase the efficacy of the restoration technologies based on cyanobacterial inoculation, especially when choosing species able to survive under these stressful conditions. Therefore, as the degradation changes the cyanobacterial community composition in biocrusts, the selection of the strains to be inoculated should be based, not only on representativeness of natural populations (Giraldo-Silva et al. 2018), but also on their capacity to survive in degraded soils. In addition, these results suggest that the restoration process of degraded soils could consist on a first inoculation with pioneer cyanobacteria, such as *L. frigida* or *T. desertorum*, followed by a second inoculation with heterocystous cyanobacteria. Finally, further analyses evaluating if the cyanobacterial community composition changes differently depending on the degradation process, would be also desirable for a more accurate restoration of different areas.

Conclusions

This study of cyanobacterial biocrust communities in different areas of southeastern Spain showed differences in taxonomic composition and specific richness, which were related to the degradation level of the sampling site, with richness becoming lower as site degradation increased. Moreover, we propose an alternative successional sequence for dryland biocrusts. The main findings support the occurrence of *Leptolyngbya frigida* in semiarid ecosystems and its dominance with *Trichocoleus desertorum* in more degraded sites, with hardly edaphic development usually covered by incipient biocrusts. Other cyanobacteria showing an increase in their abundance with degradation but specially in sites covered by more developed biocrusts were the heterocystous *Scytonema* sp., *Tolypothrix distorta* and *Nostoc commune*. However, the bundle-forming *Microcoleus* spp., and the heterocystous *Scytonema hyalinum* and *Macrochaete lichenoides* were more abundant in less degraded soils. The cyanobacteria living in the most degraded area were those able to survive in extreme conditions, and therefore able to be first colonizers of bare soil. These results show that the degradation level of the biocrust sampling site should be considered when analyzing the cyanobacterial community composition. Furthermore, the information provided in this study is of interest for a more adequate selection of cyanobacterial species to produce an inoculum that increases the success of soil restoration in drylands depending on factors such as the degradation level of the site to be restored.

Acknowledgements

This work was supported by the projects RESUCI (CGL2014-59946-R), the project REBIOARID (RTI2018-101921-B-I00), and the GL2013-44870-R and GL2017-6258-R

projects, all of them founded by the Spanish National Plan for Research and the European Union ERDF funds. Beatriz Roncero Ramos was supported by the foundation Tatiana Pérez de Guzmán el Bueno, under its pre-doctoral fellowship program. Sonia Chamizo and Emilio Rodríguez Caballero were supported by the Hipatia postdoctoral fellowship funded by the University of Almería. We are most grateful to Holcim-España S.A. and Estación Experimental de Zonas Áridas (Spanish Council of Research, CSIC) for collaborating in this research. Special thanks to the Viciano family, owner of El Cautivo, for permission to use their land as a scientific experimental site.

References

- Acea MJ, Prieto-Fernández A, Diz-Cid N 2003. Cyanobacterial inoculation of heated soils: Effect on microorganisms of C and N cycles and on chemical composition in soil surface. *Soil Biology and Biochemistry* 35,513-524
- Adams DG, Duggan PS 1999. Tansley Review No. 107. Heterocyst and akinete differentiation in cyanobacteria. *New Phytologist* 144,3-33
- Adessi A, Cruz de Carvalho R, De Philippis R, Branquinho C, Marques da Silva J 2018. Microbial extracellular polymeric substances improve water retention in dryland biological soil crusts. *Soil Biology and Biochemistry* 116,67-69
- Baran R et al. 2015. Exometabolite niche partitioning among sympatric soil bacteria. *Nature Communications* 6,8289
- Baumann K et al. 2018. Biological soil crusts along a climatic gradient in Chile: Richness and imprints of phototrophic microorganisms in phosphorus biogeochemical cycling. *Soil Biology and Biochemistry* 127,286-300
- Becerra-Absalón I, Muñoz-Martín MA, Montejano G, Mateo P 2019. Differences in the Cyanobacterial Community Composition of Biocrusts From the Drylands of Central Mexico. Are There Endemic Species? *Frontiers in Microbiology*, 10, 937
- Belnap J, Philips SL, Witwicki DL, Miller E 2008. Visually assessing the level of development and soil surface stability of cyanobacterially dominated biological soil crusts. *Journal of Arid Environments* 72, 1257-1564
- Belnap J, Weber B, Büdel B 2016. Biological Soil Crusts as an Organizing Principle in Drylands. In: Weber B, Büdel B, Belnap J eds. *Biological Soil Crusts: An Organizing Principle in Drylands*. Springer International Publishing, Cham, pp 3-13.
- Beraldi-Campesi H, Hartnett HE, Anbar A, Gordon GW, Garcia-Pichel F 2009. Effect of biological soil crusts on soil elemental concentrations: implications for biogeochemistry and as traceable biosignatures of ancient life on land. *Geobiology* 7,348-359
- Boutte C, Grubisic S, Balthasart P, Wilmotte A 2006. Testing of primers for the study of cyanobacterial molecular diversity by DGGE. *Journal of Microbiological Methods* 65,542-550

657 Cano-Díaz C, Mateo P, Muñoz-Martín MÁ, Maestre FT 2018. Diversity of biocrust-forming
658 cyanobacteria in a semiarid gypsiferous site from Central Spain. *Journal of Arid Environments*
659 151,83-89

660 Cantón Y, Domingo F, Solé-Benet A, Puigdefábregas J 2001. Hydrological and erosion
661 response of a badlands system in semiarid SE Spain. *Journal of Hydrology* 252,65-84

662 Cantón Y, Solé-Benet A, Lázaro R 2003. Soil-geomorphology relations in gypsiferous materials
663 of the tabernas desert Almería, SE Spain. *Geoderma* 115,193-222

664 Cantón Y, Del Barrio G, Solé-Benet A, Lázaro R 2004. Topographic controls on the spatial
665 distribution of ground cover in the Tabernas badlands of SE Spain. *Catena* 55,341–365

666 Cantón Y, Román JR, Chamizo S, Rodríguez-Caballero E, Moro MJ 2014. Dynamics of organic
667 carbon losses by water erosion after biocrust removal. *Journal of Hydrology and*
668 *Hydromechanics* 62,258-268

669 Cantón Y, Chamizo S, Rodríguez-Caballero E, Lázaro R, Roncero-Ramos B, Román JR, Solé-
670 Benet A 2020. Water Regulation in Cyanobacterial Biocrusts from Drylands: Negative Impacts
671 of Anthropogenic Disturbance. *Water* 12, 720

672 Capkova K, Hauer T, Rehakova K, Dolezal J 2016. Some Like it High! Phylogenetic Diversity
673 of High-Elevation Cyanobacterial Community from Biological Soil Crusts of Western
674 Himalaya. *Microbial Ecology* 71,113-123

675 Caporaso JG et al. 2010. QIIME allows analysis of high-throughput community sequencing
676 data. *Nature Methods* 7,335-336

677 Chamizo S, Cantón Y, Lázaro R, Solé-Benet A, Domingo F 2012. Crust Composition and
678 Disturbance Drive Infiltration Through Biological Soil Crusts in Semiarid Ecosystems
679 *Ecosystems* 15,148-161

680 Chamizo S, Cantón Y, Rodríguez-Caballero E, Domingo F 2016. Biocrusts positively affect the
681 soil water balance in semiarid ecosystems. *Ecohydrology* 9,1208-1221

682 Chamizo S, Rodríguez-Caballero E, Román JR, Cantón Y 2017. Effects of biocrust on soil
683 erosion and organic carbon losses under natural rainfall. *Catena* 148,117-125

684 Chamizo S, Mugnai G, Rossi F, Certini G, De Philippis R 2018. Cyanobacteria inoculation
685 improves soil stability and fertility on different textured soils: Gaining insights for applicability
686 in soil restoration. *Frontiers in Environmental Science* 6

687 Chen L, Xie Z, Hu C, Li D, Wang G, Liu Y 2006. Man-made desert algal crusts as affected by
688 environmental factors in Inner Mongolia, China. *Journal of Arid Environments* 67,521-527

689 Chilton AM, Neilan BA, Eldridge DJ 2017. Biocrust morphology is linked to marked
690 differences in microbial community composition. *Plant and Soil* 1-11

691 Couradeau E, Karaoz U, Lim HC, Nunes da Rocha U, Northen T, Brodie E, Garcia-Pichel F
692 2016. Bacteria increase arid-land soil surface temperature through the production of sunscreens.
693 *Nature Communications* 7,10373

694 Crittenden PD, Llimona X, Sancho LG 2007. Lichenized unicellular cyanobacteria fix nitrogen
695 in the light. *Canadian Journal of Botany* 85,1003-1006

696 del Barrio G, Puigdefabregas J, Sanjuan ME, Stellmes M, Ruiz A 2010. Assessment and
697 monitoring of land condition in the Iberian Peninsula, 1989–2000. *Remote Sensing of*
698 *Environment* 114,1817-1832

699 Delgado-Baquerizo M, Maestre F, Gallardo A et al 2013. Decoupling of soil nutrient cycles as a
700 function of aridity in global drylands. *Nature* 502, 672–676

701 Dojani S, Büdel B, Deutschewitz K, Weber B 2011. Rapid succession of Biological Soil Crusts
702 after experimental disturbance in the Succulent Karoo, South Africa. *Applied Soil Ecology*
703 48,263-269

704 Dojani S, Kauff F, Weber B, Budel B 2014. Genotypic and phenotypic diversity of
705 cyanobacteria in biological soil crusts of the Succulent Karoo and Nama Karoo of southern
706 Africa. *Microbial Ecology* 67,286-301

707 Edgar RC 2010. Search and clustering orders of magnitude faster than BLAST. *Bioinformatics*
708 26,2460-2461

709 Edgar RC 2013. UPARSE: Highly accurate OTU sequences from microbial amplicon reads.
710 *Nature Methods* 10, 996-998

711 Felsenstein J. 1985. Confidence limits on phylogenies: an approach using the bootstrap.
712 *Evolution* 39, 783-791

713 Fernandes VMC, Machado de Lima NM, Roush D, Rudgers J, Collins SL, Garcia-Pichel F
714 2018. Exposure to predicted precipitation patterns decreases population size and alters
715 community structure of cyanobacteria in biological soil crusts from the Chihuahuan Desert.
716 *Environmental Microbiology* 20, 259-269

717 Fewer D, Friedl T, Büdel B 2002. Chroococciopsis and Heterocyst-Differentiating
718 Cyanobacteria Are Each Other's Closest Living Relatives. *Molecular Phylogenetics and*
719 *Evolution* 23, 82-90

720 García-Ávalos S, Rodríguez-Caballero E, Miralles I, Luna L, Domene MA, Solé-Benet A,
721 Cantón Y 2018. Water harvesting techniques based on terrain modification enhance vegetation
722 survival in dryland restoration. *Catena* 167

723 Garcia-Pichel F, Castenholz RW 1991. Characterization and biological implications of
724 scytonemin, a cyanobacterial sheath pigment. *Journal of Phycology* 27, 395-409

725 Garcia-Pichel F, Lopez-Cortes A, Nubel U 2001. Phylogenetic and morphological diversity of
726 cyanobacteria in soil desert crusts from the Colorado plateau. *Applied Environmental*
727 *Microbiology* 67, 1902-1910

728 Garcia-Pichel F, Loza V, Marusenko Y, Mateo P, Potrafka RM 2013. Temperature drives the
729 continental-scale distribution of key microbes in topsoil communities. *Science* 340, 1574-1577

730 Garcia-Pichel F, Wojciechowski MF 2009. The evolution of a capacity to build supra-cellular
731 ropes enabled filamentous cyanobacteria to colonize highly erodible substrates. *PLoS One* 4,
732 e7801

733 Gee GW, Bauder JW 1986. Particle-size analysis. In: Klute A ed. *Methods of Soil Analysis*,
734 part I. Physical and Mineralogical Methods, 2nd edition. Agronomy, vol. 9. American Society
735 of Agronomy, Madison, Wi, pp. 383–411

736 Giraldo-Silva A, Nelson C, Barger NN, Garcia-Pichel F 2018. Nursing biocrusts: isolation,
737 cultivation and fitness test of indigenous cyanobacteria. *Restoration Ecology*

738 Gypser S, Herppich WB, Fischer T, Lange P, Veste M 2016. Photosynthetic characteristics and
739 their spatial variance on biological soil crusts covering initial soils of post-mining sites in Lower
740 Lusatia, NE Germany. *Flora - Morphology, Distribution, Functional Ecology of Plants* 220,
741 103-116.

742 Gu Z, Gu L, Eils R, Schlesner M, Brors B 2014. circlize implements and enhances circular
743 visualization in R. *Bioinformatics* 30, 2811-2812

744 Hu C, Liu Y, Song L, Zhang D 2002. Effect of desert soil algae on the stabilization of fine
745 sands. *Journal of Applied Phycology* 14, 281-292

746 Hu C, Gao K, Whitton BA 2012. Semi-arid regions and deserts, in *Ecology of Cyanobacteria II*,
747 ed. B. Whitton Dordrecht: Springer., 345–369

748 Jung P, Briegel-Williams L, Schermer M, Büdel B 2018. Strong in combination: Polyphasic
749 approach enhances arguments for cold-assigned cyanobacterial endemism *MicrobiologyOpen*

750 Jungblut AD, Lovejoy C, Vincent WF 2009. Global distribution of cyanobacterial ecotypes in
751 the cold biosphere. *The Isme Journal* 4, 191

752 Kumar D, Adhikary SP 2014. Diversity, molecular phylogeny, and metabolic activity of
753 cyanobacteria in biological soil crusts from Santiniketan India.. *Journal of Applied Phycology*
754 27, 339-349

755 Kumar S, Nei M, Dudley J, Tamura K 2008. MEGA: A biologist-centric software for
756 evolutionary analysis of DNA and protein sequences. *Briefings in Bioinformatics* 9, 299-306

757 Kuske CR, Yeager CM, Johnson S, Ticknor LO, Belnap J 2012. Response and resilience of soil
758 biocrust bacterial communities to chronic physical disturbance in arid shrublands. *ISME Journal*
759 6, 886-897

760 Lanzén A et al. 2012. CREST – Classification Resources for Environmental Sequence Tags.
761 *PLOS ONE* 7, e49334

762 Lázaro R, Cantón Y, Solé-Benet A, Bevan J, Alexander R, Sancho LG, Puigdefábregas J 2008.
763 The influence of competition between lichen colonization and erosion on the evolution of soil
764 surfaces in the Tabernas badlands SE Spain. and its landscape effects. *Geomorphology* 102,
765 252-266

766 Luna L, Miralles I, Andrenelli MC, Gisbert M, Pellegrini S, Vignozzi N, Solé-Benet A 2016.
767 Restoration techniques affect soil organic carbon, glomalin and aggregate stability in degraded
768 soils of a semiarid Mediterranean region. *Catena* 143, 256-264

769 Luna L, Pastorelli R, Bastida F, Hernández T, García C, Miralles I, Solé-Benet A 2016b. The
770 combination of quarry restoration strategies in semiarid climate induces different responses in
771 biochemical and microbiological soil properties. *Applied Soil Ecology* 107, 33-47

772 Maier S, Tamm A, Wu D, Caesar J, Grube M, Weber B 2018. Photoautotrophic organisms
773 control microbial abundance, diversity, and physiology in different types of biological soil
774 crusts. *The ISME Journal* 12, 1032–1046

775 Mingorance MD, Barahona E, Fernández-Gálvez J 2007. Guidelines for improving organic
776 carbon recovery by the wet oxidation method. *Chemosphere* 68, 409-413

777 Miralles I, van Wesemael B, Cantón Y, Chamizo S, Ortega R, Domingo F, Almendros G 2012.
778 Surrogate descriptors of C-storage processes on crusted semiarid ecosystems. *Geoderma* 189-
779 190, 227-235

780 Mogul R et al. 2017. Microbial Community and Biochemical Dynamics of Biological Soil
781 Crusts across a Gradient of Surface Coverage in the Central Mojave Desert. *Frontiers in*
782 *Microbiology* 8, 1974

783 Mora JL, Lázaro R 2013. Evidence of a threshold in soil erodibility generating differences in
784 vegetation development and resilience between two semiarid grasslands. *Journal of Arid*
785 *Environments* 89, 57-66

786 Mora JL, Lázaro R 2014. Seasonal changes in bulk density under semiarid patchy vegetation:
787 the soil beats. *Geoderma* 235-236, 30-38

788 Moreno-Jiménez E, Plaza C, Saiz H, Manzano R, Flagmeier M, Maestre FT 2019. Aridity and
789 reduced soil micronutrient availability in global drylands. *Nature Sustainability* 2, 371–377

790 Mugnai G et al. 2018. Development of the polysaccharidic matrix in biocrusts induced by a
791 cyanobacterium inoculated in sand microcosms. *Biology and Fertility of Soils* 54, 27-40

792 Mühlsteinová R, Johansen JR, Pietrasiak N, Martin MP, Osorio-Santos K, Warren SD 2014.
793 Polyphasic characterization of *Trichocoleus desertorum* sp. nov. *Pseudanabaenales*,
794 *Cyanobacteria*. from desert soils and phylogenetic placement of the genus *Trichocoleus*.
795 *Phytotaxa* 163, 241-261

796 Muñoz-Martín MÁ, Becerra-Absalón I, Perona E, Fernández-Valbuena L, Garcia-Pichel F,
797 Mateo P 2019. Cyanobacterial biocrust diversity in Mediterranean ecosystems along a
798 latitudinal and climatic gradient. *New Phytologist* 22, 123-141

799 Muñoz-Rojas M, Román JR, Roncero-Ramos B, Erickson TE, Merritt DJ, Aguila-Carricondo P,
800 Cantón Y 2018. Cyanobacteria inoculation enhances carbon sequestration in soil substrates used
801 in dryland restoration. *Science of the Total Environment* 636, 1149-1154

802 Navas-Molina JA, Peralta-Sanchez JM, Gonzalez A, McMurdie PJ, Vazquez-Baeza Y, Xu Z,
803 Ursell LK, Lauber C, Zhou H, Song SJ et al. 2013. Advancing our understanding of the human
804 microbiome using QIIME. *Methods in Enzymology* 531, 371–444

805 Nubel U, Garcia-Pichel F, Muyzer G 1997. PCR primers to amplify 16S rRNA genes from
806 cyanobacteria Appl Environ Microbiol 63, 3327-3332

807 Oksanen J, Blanchet FG, Friendly M, Kindt R, Legendre P, McGlinn D, Minchin PR, O'Hara
808 RB, Simpson GL, Solymos P et al 2014. Package vegan: community ecology package.

809 Patzelt DJ, Hodač L, Friedl T, Pietrasiak N, Johansen JR 2014. Biodiversity of soil
810 cyanobacteria in the hyper-arid Atacama Desert, Chile. Journal of Phycology 50, 698-710

811 Pinder JE, Kroh GC, White JD, Basham May AM 1997. The relationships between vegetation
812 type and topography in Lassen Volcanic National Park. Plant Ecology 131, 17-29

813 Podda F, Medas D, De Giudici G, Ryszka P, Wolowski K, Turnau K 2014. Erratum to: Zn
814 biomineralization processes and microbial biofilm in a metal-rich stream Naracauli, Sardinia..
815 Environmental Science and Pollution Research 21, 6809-6811

816 Pushkareva E, Pessi IS, Wilmotte A, Elster J 2015. Cyanobacterial community composition in
817 Arctic soil crusts at different stages of development. FEMS Microbiology Ecology 91

818 Pylro VS, Roesch LFW, Morais DK, Clark IM, Hirsch PR, Tótola MR 2014. Data analysis for
819 16S microbial profiling from different benchtop sequencing platforms. Journal of
820 Microbiological Methods 107, 30-37

821 R Core Team 2017. R: A language and environment for statistical computing. R Foundation for
822 Statistical Computing. Vienna, Austria.

823 Rajeev L et al. 2013. Dynamic cyanobacterial response to hydration and dehydration in a desert
824 biological soil crust. The ISME Journal 7, 2178-2191

825 Řeháková K, Johansen JR, Casamatta DA, Xuesong L, Vincent J 2007. Morphological and
826 molecular characterization of selected desert soil cyanobacteria: three species new to science
827 including Mojavia pulchra gen. et sp. Nov. Phycologia 46, 481-502

828 Rey A, Pegoraro E, Oyonarte C, Were A, Escribano P, Raimundo J 2011. Impact of land
829 degradation on soil respiration in a steppe Stipa tenacissima L. semi-arid ecosystem in the SE of
830 Spain. Soil Biology and Biochemistry 43, 393-403

831 Rodríguez-Caballero E, Knerr T, Weber B 2015. Importance of biocrusts in dryland monitoring
832 using spectral indices. Remote Sensing of Environment 170, 32-39

833 Rodríguez-Caballero E, Belnap J, Büdel B, Crutzen PJ, Andreae MO, Pöschl U, Weber B 2018.
834 Dryland photoautotrophic soil surface communities endangered by global change. Nature
835 Geoscience 11, 185-189

836 Román JR, Roncero-Ramos B, Chamizo S, Rodríguez-Caballero E, Cantón Y 2018. Restoring
837 soil functions by means of cyanobacteria inoculation: Importance of soil conditions and species
838 selection. Land Degradation and Development 29, 3184-3193

839 Roncero-Ramos B, Muñoz-Martín MA, Chamizo S, Fernández-Valvueda L, Mendoza D,
840 Perona E, Cantón Y, Mateo P 2019. Polyphasic evaluation of key cyanobacteria in biocrusts
841 from the most arid region in Europe. PeerJ 7, e6169

842 Rosario LP, del Barrio G, Sanjuan ME, Ruiz A, Martinez-Valderrama J, Puigdefabregas J 2015.
843 Prioridades de aplicação do Programa de Ação Nacional de Combate à Desertificação com base
844 nas condições do solo. In: Figueiredo TD, Fonseca F, Nunes L eds. Proteção do Solo e Combate
845 à Desertificação: oportunidade para as regiões transfronteiriças. Instituto Politécnico de
846 Bragança, Bragança, pp 47-60

847 Rossi F, De Philippis R 2015. Role of cyanobacterial exopolysaccharides in phototrophic
848 biofilms and in complex microbial mats. *Life* 5, 1218-1238

849 Rossi F, Li H, Liu Y, De Philippis R 2017. Cyanobacterial inoculation cyanobacterisation.:
850 Perspectives for the development of a standardized multifunctional technology for soil
851 fertilization and desertification reversal. *Earth-Science Reviews* 171, 28-43

852 Rossi F, Mugnai G, De Philippis R 2018. Complex role of the polymeric matrix in biological
853 soil crusts. *Plant and Soil* 429, 19-34

854 Sanjuán ME, del Barrio G, Ruiz A, Puigdefábregas J 2013. Mapa de la Condición de la Tierra
855 en España Memoria Estación Experimental de Zonas Áridas (CSIC), Almería pp 78

856 Schopf JW 2013. The fossil record of cyanobacteria. In: *Ecology of Cyanobacteria II: Their*
857 *Diversity in Space and Time.* pp 15-36

858 Siciliano SD, Palmer AS, Winsley T, Lamb E, Bissett A, Brown MV, Dorst J, Ji M, Ferrari BC,
859 Grogan P, Chu H, Snape I 2014. Soil fertility is associated with fungal and bacterial richness,
860 whereas pH is associated with community composition in polar soil microbial communities.
861 *Soil Biology and Biochemistry* 78, 10-20

862 Snedecor GW, Cochran WG 1984. *Métodos Estadísticos.* C.E.C.S.A, México

863 Steel RGD, Torrie JH 1980. *Principles and Procedures of Statistics*, 2nd ed. McGraw-Hill Book
864 Co., New York

865 Steel RGD, Torrie JH 1985. *Bioestadística: Principios y Procedimientos.* McGraw-Hill, Bogotá

866 Steven B, Belnap J, Kuske CR 2018. Chronic physical disturbance substantially alters the
867 response of biological soil crusts to a wetting pulse, as characterized by metatranscriptomic
868 sequencing. *Frontiers in Microbiology* 9

869 Steven B, Gallegos-Graves LV, Belnap J, Kuske CR 2013. Dryland soil microbial communities
870 display spatial biogeographic patterns associated with soil depth and soil parent material. *FEMS*
871 *Microbiology Ecology* 86, 101-113

872 Tajima F, Nei M 1984. Estimation of evolutionary distance between nucleotide sequences
873 *Molecular Biology and Evolution* 1, 269-285

874 Taton A, Grubisic S, Ertz D, Hodgson DA, Piccardi R, Biondi N, Tredici MR, Mainini M, Losi
875 D, Marinelli F 2006. Polyphasic study of antarctic cyanobacterial strains. *Journal of Phycology*
876 42, 1257-1270

877 Tucker CJ 1979. Red and photographic infrared linear combinations for monitoring vegetation.
878 *Remote Sensing of Environment* 8, 127-150

- 879 Velasco Ayuso S, Giraldo Silva A, Nelson C, Barger NN, Garcia-Pichel F 2017. Microbial
880 Nursery Production of High-Quality Biological Soil Crust Biomass for Restoration of Degraded
881 Dryland Soils. *Applied Environmental Microbiology* 83
- 882 Weber B, Bowker M, Zhang Y, Belnap J 2016. Natural Recovery of Biological Soil Crusts
883 After Disturbance. In: Weber B, Büdel B, Belnap J eds. *Biological Soil Crusts: An Organizing*
884 *Principle in Drylands*. Springer International Publishing, Cham, pp 479-498
- 885 Welch RM, Shuman L 1995. Micronutrient Nutrition of Plants. *Critical Reviews in Plant*
886 *Science* 14, 49–82
- 887 Whitton BA, Potts M 2012. Introduction to the cyanobacteria. In: Whitton BA ed. *Ecology of*
888 *Cyanobacteria II: Their Diversity in Space and Time*. Springer, Dordrecht Heidelberg New
889 York London, pp 1-13
- 890 Williams L, Loewen-Schneider K, Maier S, Budel B 2016. Cyanobacterial diversity of western
891 European biological soil crusts along a latitudinal gradient. *FEMS Microbiology Ecology* 92
- 892 Williams W, Büdel B, Williams S 2018. Wet season cyanobacterial N enrichment highly
893 correlated with species richness and Nostoc in the northern Australian savannah.
894 *Biogeosciences* 15, 2149-2159
- 895 Yeager CM, Kornosky JL, Housman DC, Grote EE, Belnap J, Kuske CR 2004. Diazotrophic
896 community structure and function in two successional stages of biological soil crusts from the
897 Colorado Plateau and Chihuahuan Desert. *Applied Environmental Microbiology* 70, 973-983
- 898 Yeager CM et al. 2007. Three distinct clades of cultured heterocystous cyanobacteria constitute
899 the dominant N₂-fixing members of biological soil crusts of the Colorado Plateau, USA. *FEMS*
900 *Microbiology Ecology* 60, 85-97
- 901 Yilmaz P, Parfrey LW, Yarza P, Gerken J, Pruesse E, Quast C, Schweer T, Peplies J, Ludwig
902 W, Glockner FO 2014. The SILVA and “All-species Living Tree Project LTP.” taxonomic
903 frameworks. *Nucleic Acids Research* 42, D643–D648
- 904 Zavarzina AG, Zavarzin GA 2013. Humic substances in the early biosphere. *Paleontological*
905 *Journal* 47, 984-988
- 906 Zhang YM, Wang HL, Wang XQ, Yang WQ, Zhang DY 2006. The microstructure of
907 microbiotic crust and its influence on wind erosion for a sandy soil surface in the
908 Gurbantunggut Desert of Northwestern China. *Geoderma* 132, 441-449

909

910

911

912

913 Figure captions

914 Figure 1 Phylogenetic tree based on the analysis of the 16S rRNA gene, obtained by the
915 neighbor-joining method. a) Filamentous nonheterocystous cyanobacteria and
916 unicellular/colonial cyanobacteria (collapsed). b) Several groups from tree a) expanded.
917 Numbers near nodes indicate bootstrap values greater than or equal to 50. Sequences in bold
918 were obtained from isolated cultures from biocrusts in the same experimental areas and/or from
919 other Spanish study areas.

920 Figure 2 Phylogenetic tree based on the analysis of the 16S RNA gene, obtained by the
921 neighbor-joining method, belonging to heterocystous cyanobacteria. Broken lines surrounding
922 the different clusters and their colors correspond to taxonomic assignments of Table 2 and
923 Figure 3. Numbers near nodes indicate bootstrap values greater than or equal to 50. Sequences
924 in bold were obtained from isolated cultures from biocrusts in the same experimental areas
925 and/or from other Spanish study areas.

926 Figure 3 Cyanobacterial community composition of the biocrust samples, showing the
927 percentage of reads corresponding to each OTU relative to the total number of reads per sample.
928 Each taxon is represented by a different color, and each OTU by a number, as shown in the
929 aside table. Color numbers have been changed to black or white for a better contrast with the
930 background color. Samples are ordered by decreasing degradation level from left to right.
931 Acronyms represent: IQ, MQ and DQ, respectively, incipient, medium and developed biocrusts
932 from the Gádor Quarry; IC and DC, respectively, incipient and developed biocrusts from El
933 Cautivo area; and BB, Balsa Blanca developed biocrusts

934 Figure 4 Chord-diagram representing the abundance of the main identified cyanobacterial
935 groups in biocrust samples. Soil samples are ordered by their land-condition index (or
936 degradation level) from top-left (incipient biocrusts from the Gádor quarry) to top-right
937 (developed biocrusts from the Balsa Blanca area). Major cyanobacteria groups are shown in the
938 bottom of the diagram indicated by colors as follows: heterocystous (yellow),
939 unicellular/colonial (light green), other nonheterocystous filamentous (orange), bundle-forming
940 (dark green) and unassigned OTUs (grey). Acronyms represent: IQ, MQ and DQ, respectively,
941 incipient, medium and developed biocrusts from the Gádor Quarry; IC and DC, respectively,
942 incipient and developed biocrusts from El Cautivo area; and BB, Balsa Blanca developed
943 biocrusts

944 Figure 5 Cyanobacterial richness (number of OTUs) in biocrust samples, ordered by their land-
945 condition index or degradation level (from left to right). Acronyms represent: IQ, MQ and DQ,
946 respectively, incipient, medium and developed biocrusts from the Gádor Quarry; IC and DC,
947 respectively, incipient and developed biocrusts from El Cautivo area; and BB, Balsa Blanca
948 developed biocrusts.

949 Figure 6 Heat map table showing from higher (background dark green color) to lower
950 (background yellow color) relative abundance of each taxonomic group in all biocrusts along
951 the land-condition index (or degradation level). The slope column shows the values obtained
952 from the χ^2 linear regression. The taxa whose abundance was significantly related to the land-
953 condition index are marked with an asterisk. Images show an example of the biocrust types
954 sampled per area and the UPGMA clustering of the cyanobacterial biocrust communities.
955 Distances correspond to community dissimilarities computed by the weighted-unifrac distance
956 matrix. Acronyms represent: IQ, MQ and DQ, respectively, incipient, medium and developed

957 biocrusts from the Gádor Quarry; IC and DC, respectively, incipient and developed biocrusts
958 from El Cautivo area; and BB, Balsa Blanca developed biocrusts
959

Table 1 Physicochemical soil properties and conservation index of biocrusts samples. The land-condition index values range from 0 (the most degraded site) to 1 (the less degraded site).

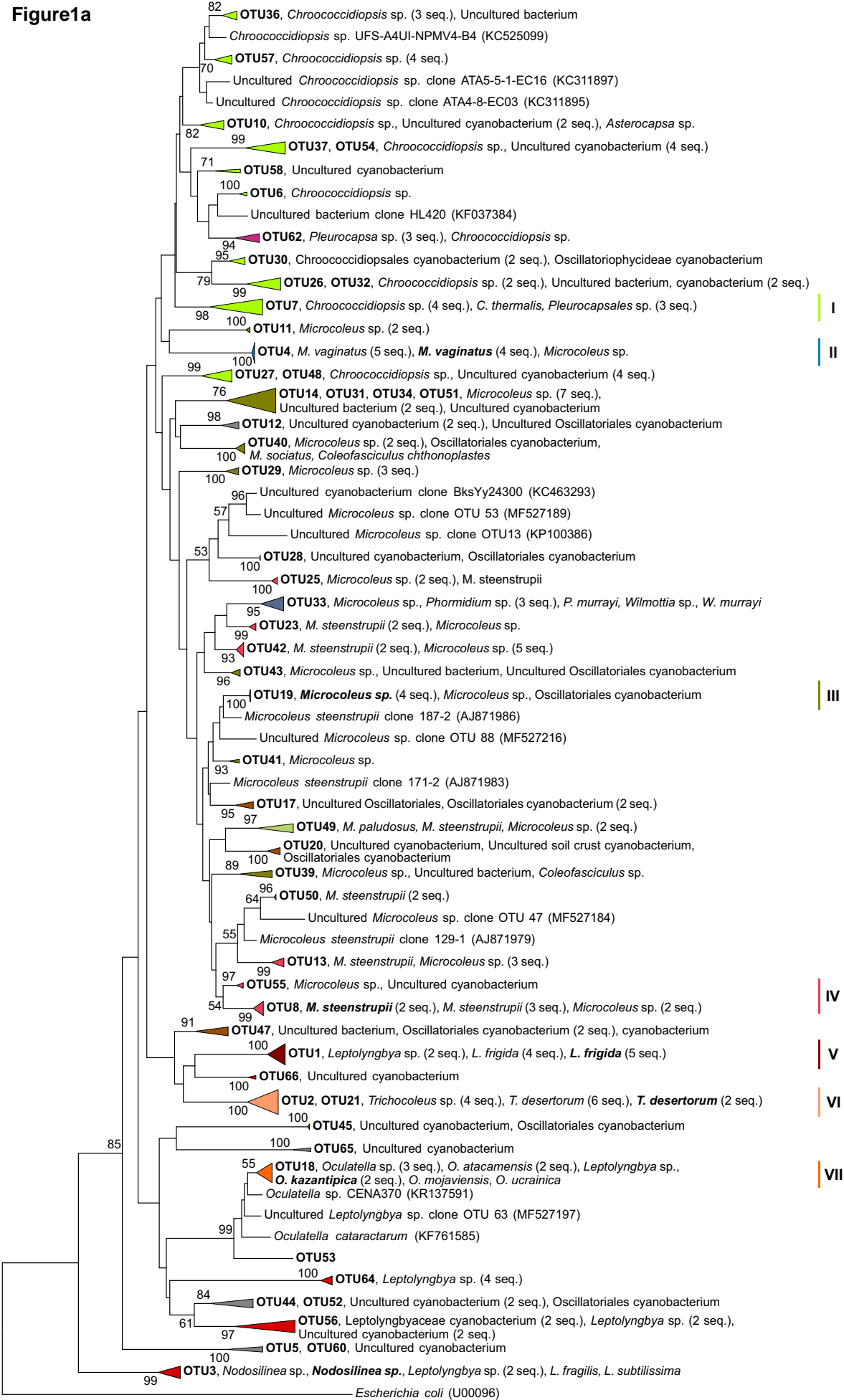
	<i>Gádor quarry</i>			<i>El Cautivo</i>		<i>Balsa Blanca</i>
<i>Biocrust development</i>	Incipient	Medium	Developed	Incipient	Developed	Developed
<i>Land-condition index</i>	0.36	0.38	0.40	0.48	0.61	0.95
<i>Texture</i>	Loam		Silty loam		Sandy loam	
<i>Sand (%)</i>	32.70	33.90	18.09	23.95	28.07	62.84
<i>Silt (%)</i>	41.57	44.71	61.68	57.27	56.38	24.10
<i>Clay (%)</i>	25.73	21.38	20.23	18.79	15.55	13.06
<i>Gravel (%)</i>	9.90	14.60	13.16	3.09	2.91	10.19
<i>OC (g·kg⁻¹)</i>	2.10	5.12	5.23	7.44	10.03	17.97
<i>Total N (g·kg⁻¹)</i>	0.45	0.64	0.77	0.82	1.53	1.72
<i>C/N</i>	4.66	8.00	6.79	9.08	6.55	10.45
<i>Sulfate (Gypsum) (%)</i>	0.0045	0.0045	0.0361	0.0062	0.0045	0.0050
<i>Conductivity (S·m⁻¹)</i>	0.18	0.10	0.20	0.10	0.10	0.12
<i>Cl (cmol·kg⁻¹)</i>	0.37	0.07	0.07	0.07	0.07	0.07
<i>K (cmol·kg⁻¹)</i>	0.43	0.26	0.41	0.55	0.42	1.01
<i>Ca (cmol·kg⁻¹)</i>	22.6	13.1	11.4	8.3	8.3	12.3
<i>Mg (cmol·kg⁻¹)</i>	3.35	1.66	2.73	0.85	0.73	1.12
<i>Cu (mg·kg⁻¹)</i>	0.36	0.25	0.41	0.50	0.60	0.42
<i>Fe (mg·kg⁻¹)</i>	3.50	2.23	3.92	2.81	3.12	4.94
<i>Mn (mg·kg⁻¹)</i>	2.19	2.66	5.00	4.00	4.70	10.80
<i>Zn (mg·kg⁻¹)</i>	0.20	0.25	0.20	0.31	0.21	1.00

Table 2 Taxonomic assignments of the OTUs. Acronyms in column area represent: BB, Balsa Blanca developed biocrusts; IQ, MQ and DQ, respectively, incipient, medium and developed biocrusts from the Gádor Quarry; IC and DC, respectively, incipient and developed biocrusts from El Cautivo area.

OTU	Taxonomic assignment	Best match; Accession number; % similarity; Source	Area
1	<i>Leptolyngbya frigida</i>	<i>Leptolyngbya frigida</i> CAU11 Clone 2; MG641933; 100	All samples
2	<i>Trichocoleus desertorum</i>	<i>Trichocoleus desertorum</i> CAU7 Clone 1; MG641921; 97.9	All samples
3	<i>Leptolyngbya</i> sp.	<i>Leptolyngbya</i> sp. PUPCCC 112.7; KJ705098; 99.8; Blast NCBI	All samples
4	<i>Microcoleus vaginatus</i>	<i>Microcoleus vaginatus</i> COL24; KC999627; 100; Blast NCBI	All samples
5	Unassigned		All samples, except IQ
6	<i>Chroococcidiopsis</i> sp.	Uncultured <i>Chroococcidiopsis</i> sp. clone 10; MF527149; 99.3; Blast NCBI	All samples
7	<i>Chroococcidiopsis</i> sp.	Uncultured <i>Chroococcidiopsis</i> sp. clone 26; MF527164; 100; Blast NCBI	All samples
8	<i>Microcoleus steenstrupii</i>	<i>Microcoleus steenstrupii</i> CAU8 Clone 1; MG641919; 99	All samples
9	<i>Scytonema hyalinum</i>	<i>Scytonema hyalinum</i> copy-1 CAU4; MG641903; 100	All samples
10	<i>Chroococcidiopsis</i> sp.	Uncultured <i>Chroococcidiopsis</i> sp. clone 68; MF527201; 99.8; Blast NCBI	All samples, except IQ
11	<i>Microcoleus</i> sp.	<i>Microcoleus</i> sp. MOA3-1A clone A; EU586741; 99.5; Blast NCBI	All samples, except MQ
12	Unassigned		All samples
13	<i>Microcoleus steenstrupii</i>	<i>Microcoleus steenstrupii</i> SON82; KC999635; 99.2; Blast NCBI	All samples, except IQ and MQ
14	<i>Microcoleus</i> sp.	Uncultured <i>Microcoleus</i> sp. clone 23; MF527161; 99.5; Blast NCBI	All samples, except IQ and MQ
15	<i>Tolypothrix distorta</i>	<i>Tolypothrix distorta</i> CAU13; MG641916; 99.8	All samples
16	<i>Nostoc commune</i>	<i>Nostoc commune</i> CANT2; MG641900; 100	All samples
17	Other Oscillatoriales	Oscillatoriales cyanobacterium CMT-2BRIN- NPHLC14 clone 9A; KM083599; 99.8; Blast NCBI	All samples, except IQ and MQ
18	<i>Oculatella kazantipica</i>	<i>Oculatella kazantipica</i> AM118 Clone A; MG641929; 98.1	All samples, except IQ
19	<i>Microcoleus</i> sp.	<i>Microcoleus</i> sp. AR9; MF002056; 100	All samples
20	Other Oscillatoriales	Uncultured Oscillatoriales cyanobacterium clone 87; MF527215; 98.8; Blast NCBI	All samples, except DQ
21	<i>Trichocoleus desertorum</i>	<i>Trichocoleus desertorum</i> CAU7 Clone 1; MG641921; 98.6	All samples
22	<i>Scytonema hyalinum</i>	<i>Scytonema hyalinum</i> copy-2 AM54 Clone C; MG641906; 99.8	All samples
23	<i>Microcoleus</i> sp.	Uncultured <i>Microcoleus</i> sp. clone 7; MF527146; 99.5; Blast NCBI	All samples, except IQ and IC
24	<i>Macrochaete lichenoides</i>	<i>Macrochaete lichenoides</i> SAG 32.92; KU559619; 99.8; Blast NCBI	All samples, except IQ
25	<i>Microcoleus</i> sp.	Uncultured <i>Microcoleus</i> sp. clone 16; MF527155; 100; Blast NCBI	BB and MQ
26	<i>Chroococcidiopsis</i> sp.	Uncultured <i>Chroococcidiopsis</i> sp. clone 41; MF527179; 97.8; Blast NCBI	All samples
27	<i>Chroococcidiopsis</i> sp.	Uncultured <i>Chroococcidiopsis</i> sp. clone 19; MF527158; 99.8; Blast NCBI	All samples, except IQ and BB
28	Other Oscillatoriales	Uncultured Oscillatoriales cyanobacterium clone 32; MF527170; 100; Blast NCBI	All samples, except IQ
29	<i>Microcoleus</i> sp.	Uncultured <i>Microcoleus</i> sp. clone 35; MF527173; 99.3; Blast NCBI	BB and MQ
30	<i>Chroococcidiopsis</i> sp.	Uncultured <i>Chroococcidiopsis</i> cyanobacterium clone 30; MF527168; 100; Blast NCBI	All samples
31	<i>Microcoleus</i> sp.	Uncultured <i>Microcoleus</i> sp. clone 28; MF527166; 98.1; Blast NCBI	BB, IC and DC
32	<i>Chroococcidiopsis</i> sp.	Uncultured <i>Chroococcidiopsis</i> sp. clone 41; MF527179; 99; Blast NCBI	All samples, except IQ
33	<i>Phormidium</i> sp.	Uncultured <i>Phormidium</i> sp. clone 37; MF527175; 99.5; Blast NCBI	All samples
34	<i>Microcoleus</i> sp.	Uncultured <i>Microcoleus</i> sp. clone 28; MF527166; 99; Blast NCBI	All samples, except IQ, DQ and DC
36	<i>Chroococcidiopsis</i> sp.	Uncultured <i>Chroococcidiopsis</i> sp. clone 42; MF527180; 98.3; Blast NCBI	All samples
37	<i>Chroococcidiopsis</i> sp.	Uncultured <i>Chroococcidiopsis</i> sp. clone 27; MF527165; 99.3; Blast NCBI	All samples, except IQ and MQ
38	<i>Scytonema</i> sp.	Uncultured <i>Scytonema</i> sp. clone 56; MF527192; 97.1; Blast NCBI	All samples, except MQ
39	<i>Microcoleus</i> sp.	Uncultured <i>Microcoleus</i> sp. clone 44; MF527182; 99.8; Blast NCBI	BB and MQ
40	<i>Microcoleus</i> sp.	Uncultured <i>Microcoleus</i> sp. clone 70; MF527203; 99.5; Blast NCBI	All samples, except MQ, DQ and IC
41	<i>Microcoleus</i> sp.	Uncultured <i>Microcoleus</i> sp. clone 75; MF527208; 99; Blast NCBI	All samples, except IQ, DQ and DC
42	<i>Microcoleus steenstrupii</i>	<i>Microcoleus steenstrupii</i> SON62; KC999630; 99.8; Blast NCBI	BB, IC and DC
43	<i>Microcoleus</i> sp.	Uncultured <i>Microcoleus</i> sp. clone 52; MF527188; 99.3; Blast NCBI	All samples, except IQ, DQ and DC
44	Unassigned		MQ and BB
45	Other Oscillatoriales	Uncultured Oscillatoriales cyanobacterium clone 48; MG527185; 100; Blast NCBI	BB, IC and DC
46	<i>Rivulariaceae</i>	Unknown <i>Rivulariaceae</i> genus; Crest (SILVA database) assignment and Phylogenetic tree	IC
47	Other Oscillatoriales	Uncultured Oscillatoriales cyanobacterium clone 62; MF527196; 97; Blast NCBI	All samples, except IQ, IC and DC
48	<i>Chroococcidiopsis</i> sp.	<i>Chroococcidiopsis</i> ; Crest (SILVA database)	All samples, except IQ and BB
49	<i>Microcoleus paludosus</i>	<i>Microcoleus paludosus</i> Es Yyy1400; KC463185; 99.8; Blast NCBI	BB
50	<i>Microcoleus steenstrupii</i>	<i>Microcoleus steenstrupii</i> COL121; KC999637; 99.7; Blast NCBI	All samples, except IQ
51	<i>Microcoleus</i> sp.	Uncultured <i>Microcoleus</i> sp. clone 71; MF527204; 99.5; Blast NCBI	MQ and BB
52	Unassigned		BB
53	<i>Oculatella</i> sp.	Uncultured <i>Oculatella</i> sp. clone 36; MF527174; 97; Blast NCBI	MQ and BB
54	<i>Chroococcidiopsis</i> sp.	<i>Chroococcidiopsis</i> ; Crest (SILVA database) assignment and Phylogenetic tree	All samples, except IQ and MQ
55	<i>Microcoleus</i> sp.	Uncultured <i>Microcoleus</i> sp. clone 81; MF527212; 99.3; Blast NCBI	BB and IC
56	<i>Leptolyngbya</i> sp.	Uncultured <i>Leptolyngbya</i> sp. clone 50; MF527187; 100; Blast NCBI	BB and MQ
57	<i>Chroococcidiopsis</i> sp.	Uncultured <i>Chroococcidiopsis</i> sp. clone 59; MF527194; 100; Blast NCBI	IC and DC
58	<i>Chroococcidiopsis</i> sp.	<i>Chroococcidiopsis</i> ; Crest (SILVA database) assignment and Phylogenetic tree	All samples, except BB, IQ and IC
60	Unassigned		BB
61	<i>Scytonema</i> sp.	Uncultured <i>Scytonema</i> sp. clone 56; MF527192; 99; Blast NCBI	All samples, except MQ
62	<i>Pleurocapsa</i> sp.	Uncultured <i>Pleurocapsa</i> sp. clone 33; MF527171; 99.5; Blast NCBI	All samples, except IQ, DQ and BB
63	<i>Mojavia</i> sp.	<i>Mojavia</i> sp. AR1; MF002044.1; 100	All samples
64	<i>Leptolyngbya</i> sp.	<i>Leptolyngbya</i> sp. K1.1; JF810657; 99.5; Blast NCBI	IQ
65	Unassigned		BB
66	Unassigned		BB
-	Chimera	35, 59	

Sequences in bold were obtained from isolated cultures from biocrusts in the same experimental areas and/or from other Spanish study areas

Figure1a



0.050

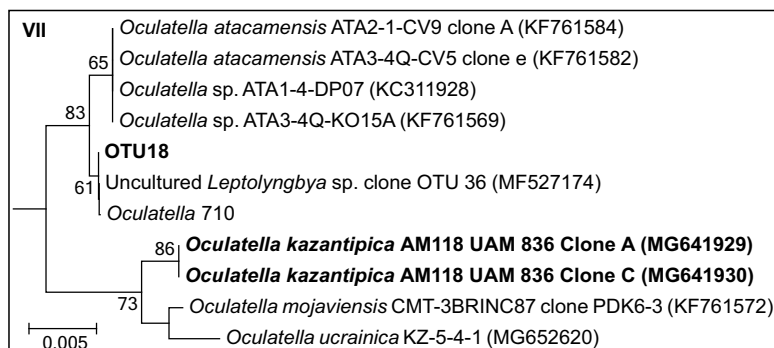
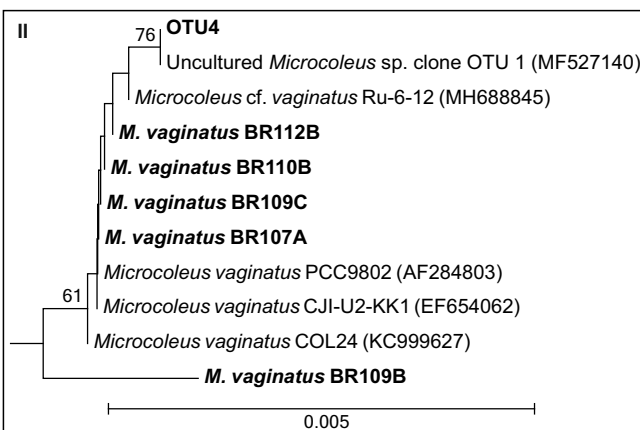
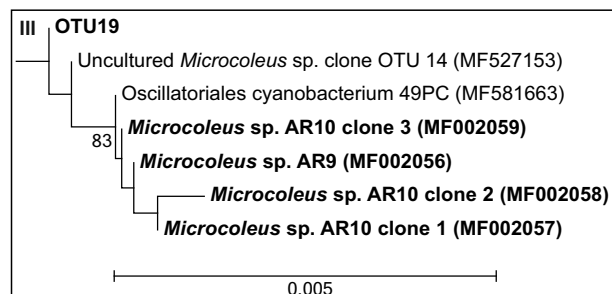
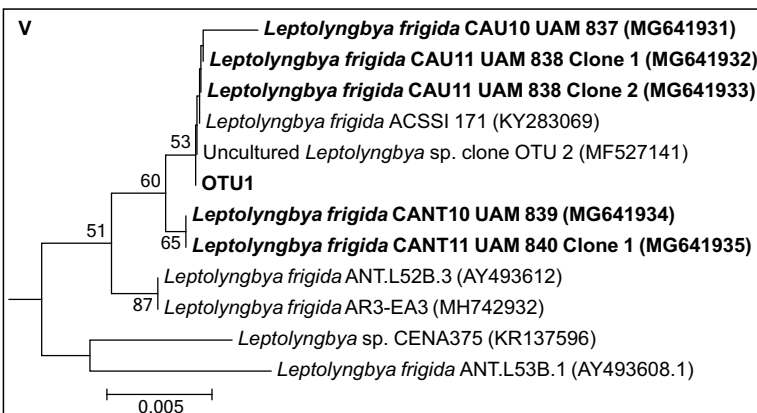
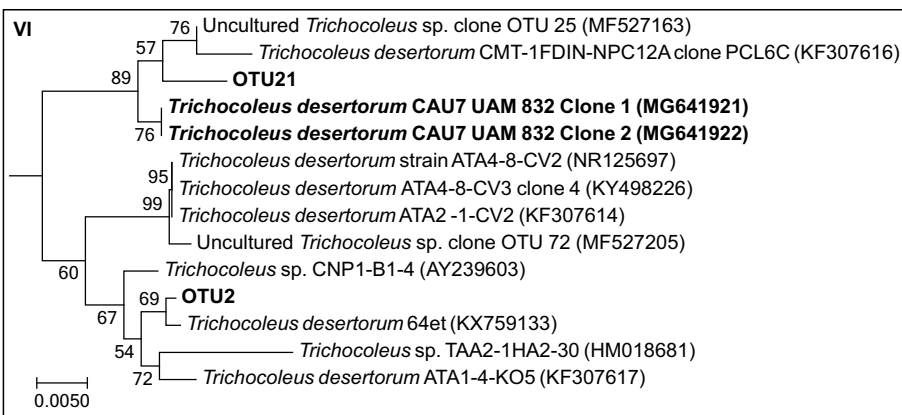
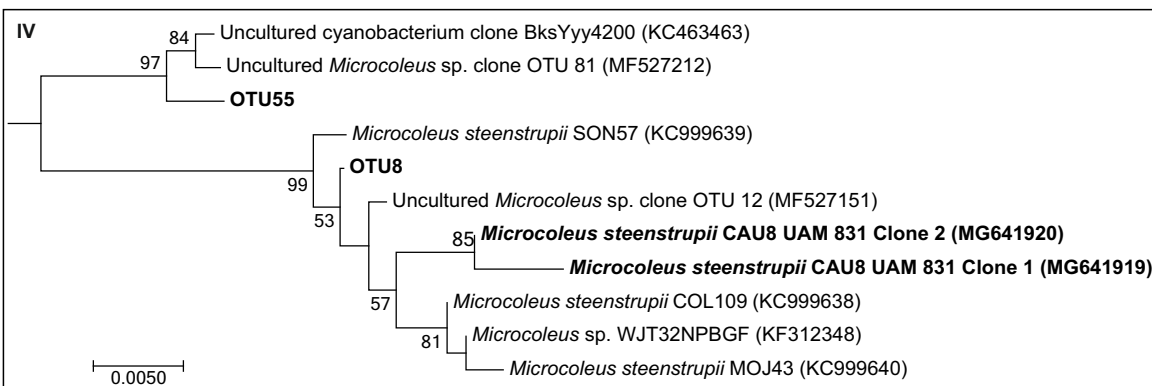
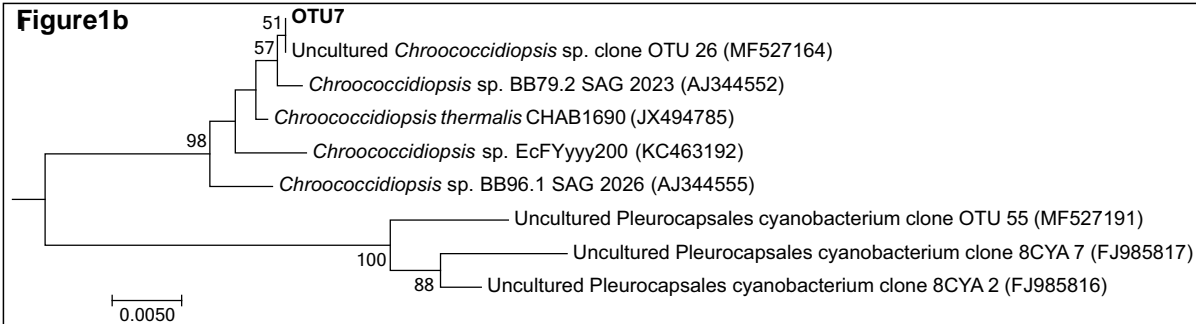


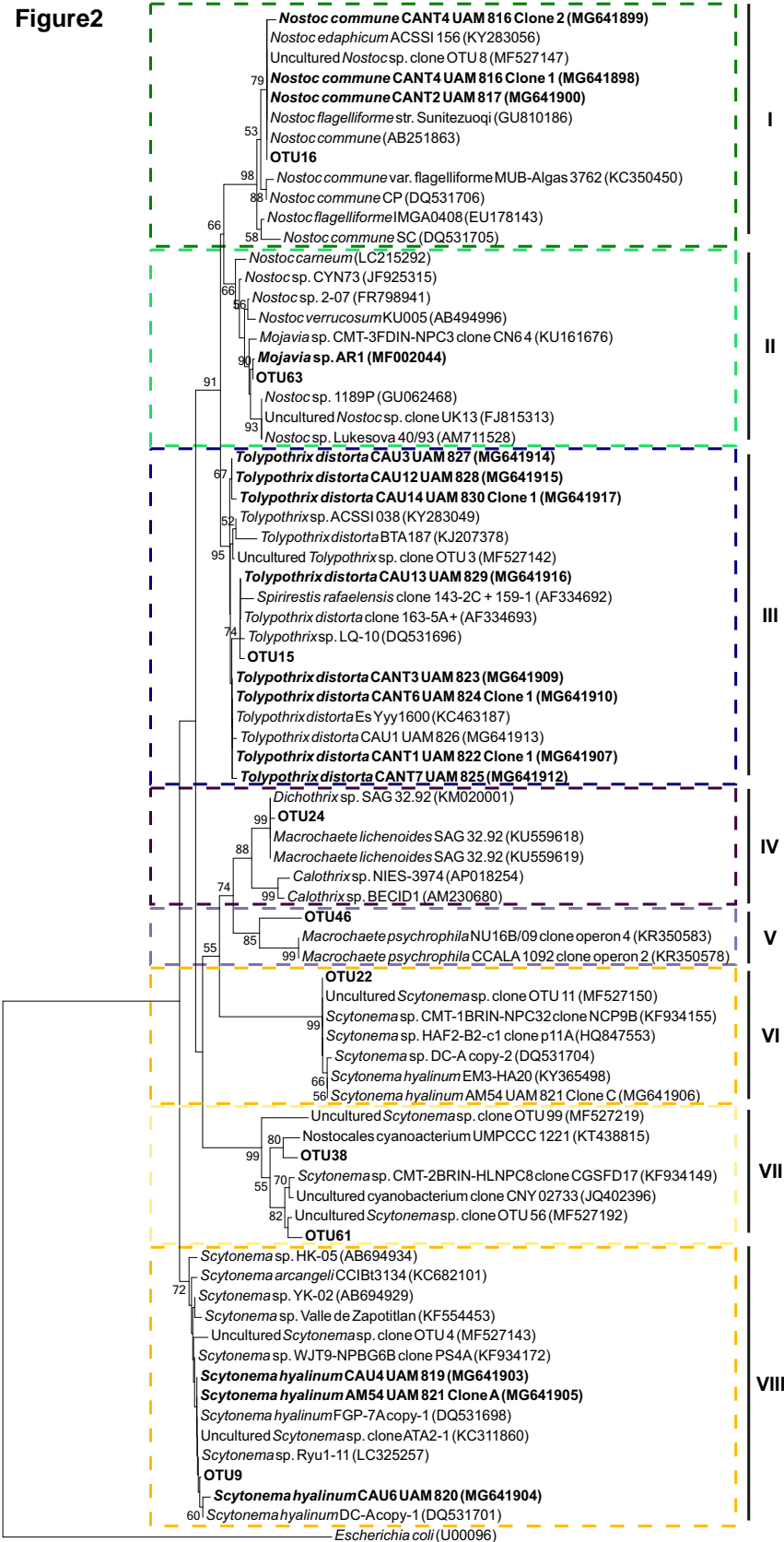
Figure2

Figure4 R1

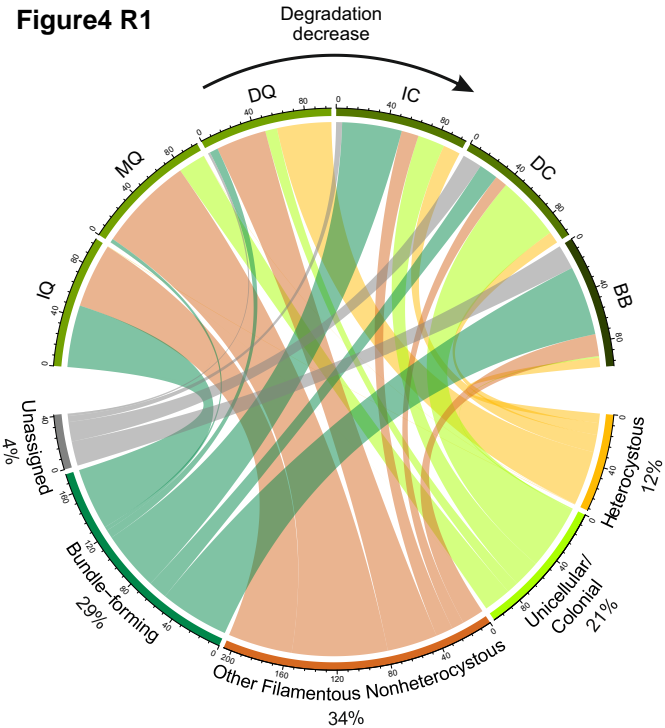


Figure5

